Adjoint-Based Adaptive Model and Discretization for Hyperbolic Systems with Relaxation

Dylan Dronnier, Florent Renac

HAL Id: hal-02179030
https://hal.science/hal-02179030

ADJOINT-BASED ADAPTIVE MODEL AND DISCRETIZATION FOR HYPERBOLIC SYSTEMS WITH RELAXATION*

DYLAN DRONNIER† AND FLORENT RENAC‡

Abstract. In this work, we use an adjoint-weighted residuals method for the derivation of an a posteriori model and discretization error estimators in the approximation of solutions to hyperbolic systems with stiff relaxation source terms and multiscale relaxation rates. These systems are parts of a hierarchy of models where the solution reaches different equilibrium states associated to different relaxation mechanisms. The discretization is based on a discontinuous Galerkin method which allows to account for the local regularity of the solution during the discretization adaptation. The error estimators are then used to design an adaptive model and discretization procedure which selects locally the model, the mesh, and the order of the approximation and balances both error components. Coupling conditions at interfaces between different models are imposed through local Riemann problems to ensure the transfer of information. The reliability of the present *hpm*-adaptation procedure is assessed on different test cases involving a Jin–Xin relaxation system with multiscale relaxation rates, and results are compared with standard *hp*-adaptation.

Key words. hyperbolic systems with relaxation sources, adjoint problem, a posteriori estimates, model adaptation, discretization adaptation, discontinuous Galerkin method

AMS subject classifications. 65N30, 65N55, 65N15

DOI. 10.1137/18M120676X

1. Introduction. We are interested in the numerical simulation of physical systems described by hyperbolic conservation laws with stiff relaxation source terms. These source terms modelize the evolution of variables toward different equilibrium states through a cascade of mechanisms. Let us quote, for instance, the modeling of two-phase flows that may involve different models [30]. The two-fluid, two-velocity, two-pressure diphasic model of Baer and Nunziato [5] treats each phase as a separate fluid with its own density, pressure, and velocity. Assuming thermal and mechanical equilibrium, one may consider drift-flux models which consist in two-fluid, one-temperature, one-pressure models [2]. Assuming kinematic equilibrium, one obtains the homogeneous (i.e., one-fluid) relaxation model, and further assuming thermodynamic equilibrium, one obtains the homogeneous equilibrium model [4]. This defines a hierarchy of models which may be selected by their corresponding characteristic relaxation time scales, and practical applications may involve heterogeneous time scales which differ by several orders of magnitude. The finer model being also the more complex one, it is legitimate to select the adapted model in regions of the flow where corresponding equilibria are achieved to lower the cost of the global simulation. This motivates the model adaptation under consideration in this work.

The different models will be separated by thin interfaces where the transfer of information should be modelized. This coupling strategy may require the numerical treatment at the interfaces of sharp relaxation layers with steep gradients of the solution, thus imposing a cumbersome resolution. In this work, the coupling will be based on the solution of a Riemann problem that allows the capture of the relaxation

---

†CERMICS, École des Ponts ParisTech, 77455 Marne la Vallée Cedex 2, France (dylan.dronnier@enpc.fr).

‡ONERA–The French Aerospace Lab, 92320 Châtillon Cedex, France (florent.renac@onera.fr).

layers and avoids their numerical resolution. We refer the reader to [3, 4, 12, 1] and references therein for a discussion on the different theoretical and numerical techniques of coupling through interfaces.

Using a model whose complexity is adapted to the local physical scales would allow a compromise between accuracy and complexity of the model. Such a strategy may be based on local error estimates and has been used in many different applications [10, 36, 35, 41, 8, 32, 14, 17]. Further allowing the local adaptation of the problem discretization would improve its flexibility and efficiency [9]. In this work, we restrict our analysis to steady-state problems and propose to derive local a posteriori estimators of both model and discretization errors on a user-defined function of interest based on the solution of an adjoint problem. Such technique provides reliable a posteriori error bounds and allows to compare both sources of error and to balance them, constituting a key advantage of the present method. The adjoint solution is used in the estimator as a weight on the residuals and gives information of the local sensitivity of the function of interest to the discretization and modelization. The error estimator is then split between local contributions to discretization and model errors where the former corresponds to the classical adjoint-weighted residuals [7, 24], while the latter consists in testing the coarse solution in the fine model.

The method may be seen as an extension to hyperbolic systems with relaxation of the work in [9] about Poisson and convection-diffusion-reaction equations. In [9], the finer models are obtained by additional terms in the equations which allow the use of a same functional space. However, in the present context the size of the state variable vector may differ between relaxation models of different complexity, which introduces some difficulty in the construction of the error estimators because the function spaces differ. We circumvent this difficulty by including the equilibrium states in the functional space through an additional constraint in the Lagrangian functional and thus use a unique framework for the derivation of the error estimators.

The error estimators are then used to propose an adaptation algorithm. Given an output functional $J(\mathbf{u})$ which depends on the solution of the fine problem, $\mathbf{u}$, the estimators provide local contributions to the error on J. The algorithm looks for an approximate solution $\mathbf{u}_{hm}$ resulting from local adaptations of both model and discretization in the whole domain. It aims at balancing both components of the error and lowering the error on J under a given tolerance

$$(1.1) \qquad |J(\mathbf{u}_{hm}) - J(\mathbf{u})| \leq \mathtt{TOL}|J(\mathbf{u}_{hm})|,$$

where $0 < \mathtt{TOL} \ll 1$ denotes the prescribed tolerance. Typical examples of functionals include global forces coefficients of a body in a fluid flow [24]. In the context of two-phase flows, this quantity could be either induced loads in propulsion systems or efficiency of cryotechnic rocket engines [33].

Let us stress that these techniques require strong regularity assumptions on the primal and dual solutions [7, 19, 36, 9]. The adjoint analysis of hyperbolic systems with discontinuous solutions indeed results in problems with systems of linear equations with discontinuous coefficients which are not well posed in general. The analysis must include the linearization of the jump relations across the discontinuity [31], which leads to a so-called interior boundary condition for the adjoint variables as shown in [42] in the context of scalar equations. In the case of systems of conservation laws, this interior boundary condition has been derived formally through stationary shocks of the compressible quasi–one-dimensional Euler equations [18]. This condition is also satisfied at the discrete level provided that the primal and dual solutions are vanishing viscosity limits of regularized problems [40]. We also refer the reader to

[23, sections 4 and 5] and the recent survey [26, section 4] and references therein for a discussion on the well-posedness of the dual problem in the presence of discontinuity of the primal solution and to [24, 23, 26, 38, 16] for numerical evidence of the sharpness and efficiency of the error indicators.

Using a Riemann problem for the coupling of different systems may also lead to nonsmooth physical solution across the coupling interface. We thus include the coupling condition as an additional constraint in the adjoint analysis which allows to linearize the systems separately where the solution is smooth. Moreover, the analysis assumes differentiability of the Riemann problem. This thus excludes coupling conditions, leading to a characteristic interface where a nonlinear wave of the solution of the Riemann problem separating discontinuous solutions has zero velocity and thus corresponds to the coupling interface.

The space discretization is based on a discontinuous Galerkin (DG) method [39, 29] which constitutes a high-order finite element method well suited to local adaptation [24, 28]. The method indeed allows to adapt either the mesh size (h-adaptation) or the approximation order of the discretization (p-adaptation) according to the local regularity of the solution. The present method thus consists in a so-called *hpm*-adaptation algorithm. The Riemann problem at coupling interfaces is also used to design a well-balanced scheme that preserves equilibrium solutions, i.e., stationary solutions satisfying the coupling conditions. Without loss of generality, we introduce the method for a hierarchy of two one-dimensional systems: the fine model and its associated equilibrium model. We use the approach based on the works of [13] and [21] (see Appendix A for details) using the solution of a local Riemann problem for the coupling of both models. Results are illustrated with a prototype defined from the framework of Jin–Xin relaxation models [27] where the corresponding equilibrium model is a nonlinear scalar equation. Numerical experiments will also be presented for this prototype.

The paper is organized as follows. Section 2 presents the different model problems and their discretizations. Subsection 2.1 introduces the hyperbolic systems with relaxation under consideration. The coupling of models through the solution of a Riemann problem is then defined in subsection 2.2, a prototype is introduced in subsection 2.3, while the space discretization with a DG method of the different systems at steady state is described in subsection 2.4. In section 4, we derive the representation of model and discretization errors based on the adjoint problem associated to the equilibrium model introduced in section 3. The adaptation algorithm is presented in section 5 and is assessed by numerical experiments in section 6. Concluding remarks about this work are given in section 7.

2. Model problem and approximation.

2.1. Hyperbolic systems with relaxation. Let $\Omega = (0, L)$ be an open interval of $\mathbb{R}$, and consider the following one-dimensional hyperbolic system:

$$(2.1) \qquad \partial_t \mathbf{u} + \partial_x \mathbf{f}(\mathbf{u}) = \tfrac{1}{\varepsilon(x)} \mathbf{s}(\mathbf{u}) \quad \text{in } \Omega \times \mathbb{R}^+.$$

The state vector $\mathbf{u} : \Omega \times \mathbb{R}^+ \ni (x, t) \mapsto \mathbf{u}(x, t) \in \mathcal{A} \subset \mathbb{R}^n$ belongs to the convex set $\mathcal{A}$ of admissible states. The flux function $\mathbf{f}$ and the source term $\mathbf{s}$, from $\mathcal{A}$ to $\mathbb{R}^n$, are supposed to be smooth. The source term modelizes some relaxation mechanisms, and $\varepsilon(\cdot) > 0$ represents a local characteristic relaxation time that may vary in different regions of the domain. We consider the case where these mechanisms depend only on

local values of the state vector. The system is closed by the initial condition,

$$(2.2) \qquad \mathbf{u}(x,0) = \mathbf{u}_0(x) \quad \forall x \in \Omega,$$

together with appropriate boundary conditions,

$$(2.3a) \qquad \mathbf{u}(0^+, t) \in \{\mathbf{w} \in \mathcal{A} : \ \mathbf{w} = \mathcal{W}_r(0^+; \mathbf{b}_0, \mathbf{u}_R) \ \forall \mathbf{u}_R \in \mathcal{A}\}, \quad \forall t > 0,$$

$$(2.3b) \qquad \mathbf{u}(L^-, t) \in \{\mathbf{w} \in \mathcal{A} : \ \mathbf{w} = \mathcal{W}_r(0^-; \mathbf{u}_L, \mathbf{b}_L) \ \forall \mathbf{u}_L \in \mathcal{A}\}, \quad \forall t > 0.$$

Here $\mathbf{b}_0$ and $\mathbf{b}_L$ are constant data in $\mathcal{A}$, and $\mathcal{W}_r(\cdot; \cdot, \cdot)$, where the subscript r stands for relaxation, denotes the solution of the Riemann problem associated to (2.1) in homogeneous form with the two last arguments as left and right initial data. We assume that the data are compatible with the existence and uniqueness of a steady-state solution to (2.1). We refer the reader to [15] or [20] for an in-depth discussion on admissible boundary conditions which is beyond the scope of the present study.

The problem defined by (2.1)–(2.3) is referred to as the *fine* model. Our goal is to compute its steady state. However, the computation might be expensive when the dimension of the state vector n is large. One way to lower its complexity is to consider a reduced model which corresponds to the limit of (2.1) when equilibrium is reached through relaxation mechanisms.

Following the framework of Chen, Levermore, and Liu [11] (see also [32]), we consider systems (2.1) of the form

$$(2.4) \qquad \begin{cases} \partial_t \mathbf{v} + \partial_x \mathbf{f}_v(\mathbf{u}) = 0, \\ \partial_t \mathbf{w} + \partial_x \mathbf{f}_w(\mathbf{u}) = \frac{1}{\varepsilon(x)}(\mathbf{w}_{eq}(\mathbf{v}) - \mathbf{w}) \end{cases} \quad \text{in } \Omega \times \mathbb{R}^+,$$

where $\mathbf{u} = (\mathbf{v}, \mathbf{w})^\top$ with $\mathbf{v}$ and $\mathbf{w}$ in suitable subsets of $\mathbb{R}^{n-k}$ and $\mathbb{R}^k$ and $\mathbf{f}(\mathbf{u}) = \left(\mathbf{f}_v(\mathbf{u}), \mathbf{f}_w(\mathbf{u})\right)^\top$ with similar dimensions. The Jacobians of the flux and source terms in (2.1) may be written as

$$(2.5) \qquad \mathbf{f}'(\mathbf{u}) = \begin{pmatrix} \partial_\mathbf{v} \mathbf{f}_v & \partial_\mathbf{w} \mathbf{f}_v \\ \partial_\mathbf{v} \mathbf{f}_w & \partial_\mathbf{w} \mathbf{f}_w \end{pmatrix}, \quad \mathbf{s}'(\mathbf{u}) = \begin{pmatrix} 0 & 0 \\ \mathbf{w}'_{eq}(\mathbf{v}) & -\mathbf{I}_{n-k} \end{pmatrix}.$$

The states $\mathbf{u}$ satisfying $\mathbf{s}(\mathbf{u}) = 0$, i.e., $\mathbf{w} = \mathbf{w}_{eq}(\mathbf{v})$, are called equilibrium states, and we denote by $\mathcal{M} := \{\mathbf{u} \in \mathcal{A} : \mathbf{s}(\mathbf{u}) = 0\}$ the equilibrium manifold. We assume that $\mathcal{M}$ can be parametrized by $\mathbf{v}$ and $\mathbf{w}_{eq}$ maps $\mathbf{v}$ to the unique $\mathbf{w}_{eq}(\mathbf{v})$ such that $\mathbf{u}_{eq}(\mathbf{v})$ belongs to $\mathcal{M}$ with

$$(2.6) \qquad \mathbf{u}_{eq}(\mathbf{v}) := \begin{pmatrix} \mathbf{v} \\ \mathbf{w}_{eq}(\mathbf{v}) \end{pmatrix}.$$

In the limit of instantaneous relaxation $\varepsilon \to 0^+$, (2.1) tends formally to the *equilibrium* model:

$$(2.7) \qquad \begin{cases} \partial_t \mathbf{v} + \partial_x \mathbf{f}_v\left(\mathbf{v}, \mathbf{w}_{eq}(\mathbf{v})\right) = 0, \\ \qquad\qquad\quad \mathbf{w} = \mathbf{w}_{eq}(\mathbf{v}) \end{cases} \quad \text{in } \Omega \times \mathbb{R}^+.$$

The adaptation method introduced in section 5 will be based on a partition of the domain Ω into a relaxation region Ω_r where the fine model holds and an equilibrium region Ω_e where the equilibrium model is applied for the global modelization of the problem. The regions satisfy

$$(2.8) \qquad \overline{\Omega} = \overline{\Omega}_r \cup \overline{\Omega}_e, \quad \Omega_r \cap \Omega_e = \emptyset,$$

and the underlying problem will be referred to as the *adapted* problem in the following. The different models are separated by thin interfaces where the transfer of information should be ensured through coupling conditions. This will be done in the next section by solving a local Riemann problem centered on the coupling interface.

2.2. The Riemann problem for coupling different models. We consider the Riemann problem defined by systems (2.4) and (2.7) in homogeneous form associated to a piecewise constant initial condition and temporarily set $\Omega = \mathbb{R}$, $\Omega_r = (-\infty, 0)$, and $\Omega_e = (0, \infty)$. Let $\mathbf{u}_L$, $\mathbf{u}_R$ in $\mathcal{A}$ be two state vectors with $\mathbf{s}(\mathbf{u}_R) = 0$. The Riemann problem consists of finding $\mathbf{u} = (\mathbf{v}, \mathbf{w})^\top$ in $\mathcal{A}$ solution of

$$(2.9a) \qquad \begin{cases} \partial_t \mathbf{v} + \partial_x \mathbf{f}_v(\mathbf{v}, \mathbf{w}) = 0, \\ \partial_t \mathbf{w} + \partial_x \mathbf{f}_w(\mathbf{v}, \mathbf{w}) = 0, \end{cases} \quad x < 0,\ t > 0,$$

$$(2.9b) \qquad \begin{cases} \partial_t \mathbf{v} + \partial_x \mathbf{f}_v(\mathbf{v}, \mathbf{w}) = 0, \\ \qquad\qquad \mathbf{w} = \mathbf{w}_{eq}(\mathbf{v}), \end{cases} \quad x > 0,\ t > 0,$$

together with the initial data,

$$(2.10) \qquad \mathbf{u}(x, 0) = \mathbf{u}_L(x), \quad x < 0, \quad \text{and} \quad \mathbf{v}(x, 0) = \mathbf{v}_R(x), \quad x > 0,$$

and suitable conditions at $x = 0$, referred to as the coupling condition and addressed later on. Introducing the orthogonal projection $\Pi_v : \mathbf{u} = (\mathbf{v}, \mathbf{w})^\top \mapsto \mathbf{v}$, we look for a function $\mathcal{W}_r^e : \mathbb{R} \times \mathcal{A} \times \Pi_v \mathcal{A} \to \mathcal{A}$ such that

$$\mathbf{u}(x, t) = \mathcal{W}_r^e \left(\tfrac{x}{t}; \mathbf{u}_L, \mathbf{v}_R \right), \quad x \in \mathbb{R}, t > 0.$$

We assume that the Riemann problem is consistent with the coupling condition:

$$(2.11) \qquad \begin{aligned} \mathbf{u}(0^-, t) &= \mathcal{W}_r^e \left(0^-; \mathbf{u}(0^-, t), \mathbf{v}(0^+, t) \right), \\ \mathbf{v}(0^+, t) &= \Pi_v \mathcal{W}_r^e \left(0^+; \mathbf{u}(0^-, t), \mathbf{v}(0^+, t) \right), \quad t > 0, \end{aligned}$$

where $\mathbf{u}(0^-, t)$ and $\mathbf{v}(0^+, t)$ are the left and right traces of the exact solution to the coupling problems (2.9) and (2.10). This property is important, as it allows the existence of steady-state solutions. We stress that from (2.9) the coupling conditions must satisfy the conservation of $\mathbf{v}$, and the Riemann problem is assumed to share this property.

In the same way, by $\mathcal{W}_e^r \left(\tfrac{x}{t}; \mathbf{v}_L, \mathbf{u}_R \right)$ we denote the solution of the Riemann problem where the models are inverted: $\Omega_r = (0, \infty)$ and $\Omega_e = (-\infty, 0)$. In the following, we further assume that $\mathcal{W}_r^e \left(0^\pm; \cdot, \cdot \right)$ and $\mathcal{W}_e^r \left(0^\pm; \cdot, \cdot \right)$ are smooth functions of their two last arguments (see Example 2), which in particular excludes conditions of characteristic coupling interfaces. Alternative approaches may be based on the approximation of the coupling conditions through the use of numerical fluxes as suggested in [1].

2.3. A Jin–Xin relaxation model as prototype. Throughout this work, we will consider an example derived from the relaxation models introduced by Jin and Xin in [27]. It is defined by the semilinear hyperbolic relaxation model:

$$(2.12) \qquad \begin{cases} \partial_t v + \partial_x w = 0, \\ \partial_t w + a^2 \partial_x v = \frac{1}{\varepsilon(x)} \left(f(v) - w \right), \end{cases}$$

where $f : \mathbb{R} \to \mathbb{R}$ is a smooth function. The characteristic variables associated to (2.12) in homogeneous form are $w \pm av$ with speeds $\pm a$, $a > 0$, satisfying the subcharacteristic condition

$$(2.13) \qquad a > |f'(v)|$$

for all the states v under consideration. We define the interval $I = (v_m, v_M)$ defined by $I := \{\, v \in \mathbb{R} \colon |f'(v)| < a \,\}$, and the admissible space $\mathcal{A}$ is a subset of $I \times f(I)$. The equilibrium model corresponding to (2.12) when ε goes to 0 is the nonlinear scalar conservation law with $f(v)$ as physical flux [34, 27].

We are now interested in v and w solutions of the adapted problem
(2.14)
$$\begin{cases} \partial_t v + \partial_x w = 0, \\ \partial_t w + a^2 \partial_x v = \frac{1}{\varepsilon}(f(v) - w) \end{cases} \text{in } \Omega_r \times \mathbb{R}^+, \quad \begin{cases} \partial_t v + \partial_x f(v) = 0, \\ w = f(v) \end{cases} \text{in } \Omega_e \times \mathbb{R}^+,$$

together with coupling conditions at the interface. We follow the work of [13] and let $\Omega_r = (0, x_c)$ and $\Omega_e = (x_c, L)$ for the sake of illustration. At steady state, w is continuous through the interface, whereas a boundary layer may appear for the v variable. The coupling conditions leading to a well-posed problem read [13]

$$(2.15) \qquad w(x_c^-, t) = f\big(v(x_c^+, t)\big), \quad v(x_c^-, t) \overset{BLN}{=} v(x_c^+, t) \quad \forall t > 0,$$

where the second equality holds in the sense of Bardos–Leroux–Nédélec (BLN) [6]:
(2.16)
$$\big(f(v(x_c^+, t)) - f(g)\big)\big(v(x_c^+, t) - v(x_c^-, t)\big) \le 0 \quad \forall t > 0, \ \forall g \in \lfloor v(x_c^-, t), v(x_c^+, t) \rceil.$$

In this work, we are interested in stationary solutions associated to boundary conditions

$$(2.17) \qquad v(0^+, t) = b_0 \in I, \quad v(L^-, t) = b_L \in I.$$

The existence and uniqueness of the entropy solution to the Cauchy problem (2.14)–(2.16) on $\mathbb{R}$ have been proved in [13] under further assumptions, while stationary solutions to the coupled problem (2.14)–(2.17) have been characterized in [21], where the Riemann problem has been solved for a convex flux f (in Appendix A we consider the case of a general flux and propose a numerical method for its resolution). In particular, the Riemann problem is proved to be consistent in the sense of (2.11): stationary solutions to the above coupled problem such that (2.15) holds satisfy

$$(2.18) \qquad \mathbf{u}(x_c^-) = \mathcal{W}_r^e\left(0^-; \mathbf{u}(x_c^-), v(x_c^+)\right), \quad v(x_c^+) = \Pi_v \mathcal{W}_r^e\left(0^+; \mathbf{u}(x_c^-), v(x_c^+)\right).$$

2.4. Space discretization. We use a DG method for the space discretization of the different problems under consideration at steady state. We first describe the space discretization of the fine problem in subsection 2.4.1 and then extend the method to the adapted one in subsection 2.4.2.

2.4.1. Space discretization of the fine problem. Let $\Omega_h = \cup_{\kappa \in \Omega_h} \kappa$ be a partition of the domain $\Omega = (0, L)$ into N elements κ. We set $x_0 = 0$, $x_N = L$ and the set of interior interfaces of the mesh $I_h := \{x_1, \dots, x_{N-1}\}$, where $x_0 < x_1 < \cdots < x_N$. Let $p : \Omega_h \to \mathbb{N}$ be a function that maps each cell of the mesh to a natural number. The DG method looks for approximate solutions in the broken polynomial space

$$(2.19) \qquad V_h := \left\{ \mathbf{v}_h \in \left(L^\infty(\Omega)\right)^n : \ \mathbf{v}_{h|\kappa} \in \left(\mathbb{P}^{p(\kappa)}(\kappa)\right)^n \quad \forall \kappa \in \Omega_h \right\},$$

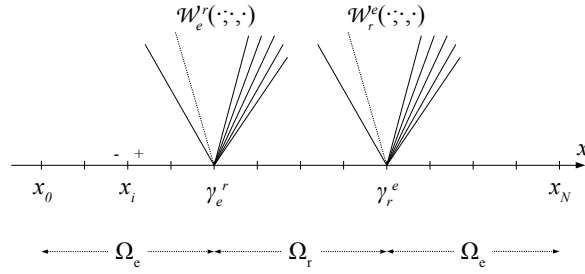where $\mathbb{P}^{p(\kappa)}(\kappa)$ is the space of polynomial functions of degree at most $p(\kappa)$ on κ.

FIG. 1. *Mesh of the adapted problem: model partition* (2.8), *interfaces, coupling interfaces, related Riemann problems (see subsection* 2.2), *and left and right traces at interfaces.*

The discretization of the fine problem is obtained by multiplying (2.1) at steady state by a test function in V_h and integrating by parts over each cell. A numerical flux is used at the interface between two cells. We thus look for a function $\mathbf{u}_h$ in V_h such that

$$(2.20) \qquad \mathcal{R}_h(\mathbf{u}_h; \boldsymbol{\psi}_h) = 0 \quad \forall \boldsymbol{\psi}_h \in V_h$$

with the semilinear form (i.e., linear in all arguments after the semicolon)

$$
\begin{aligned}
&\mathcal{R}_h(\mathbf{u}_h; \boldsymbol{\psi}_h) \\
(2.21) \qquad &:= -\int_{\Omega_h} \mathbf{f}(\mathbf{u}_h) \cdot \partial_x^h \boldsymbol{\psi}_h + \frac{1}{\varepsilon(x)} \mathbf{s}(\mathbf{u}_h) \cdot \boldsymbol{\psi}_h \, dx + \sum_{x \in I_h} \boldsymbol{\Phi}_r(\mathbf{u}_h^-, \mathbf{u}_h^+) \cdot [\![\boldsymbol{\psi}_h]\!]_x \\
&\quad - \mathbf{f}\big(\mathcal{W}_r(0^+; \mathbf{b}_0, \mathbf{u}_h(0^+))\big) \cdot \boldsymbol{\psi}_h(0^+) + \mathbf{f}\big(\mathcal{W}_r(0^-; \mathbf{u}_h(L^-), \mathbf{b}_L)\big) \cdot \boldsymbol{\psi}_h(L^-),
\end{aligned}
$$

where $\mathbf{b}_0$ and $\mathbf{b}_L$ are boundary data from (2.3). The broken derivative and jump operator are defined by $(\partial_x^h \boldsymbol{\psi}_h)_\kappa = \partial_x(\boldsymbol{\psi}_h)_\kappa$ and $[\![\boldsymbol{\psi}_h]\!]_x = \boldsymbol{\psi}_h(x^-) - \boldsymbol{\psi}_h(x^+)$, respectively, where $\boldsymbol{\psi}_h(x^-)$ and $\boldsymbol{\psi}_h(x^+)$ denote the left and right traces of $\boldsymbol{\psi}_h$ at x (see Figure 1).

The numerical flux $\boldsymbol{\Phi}_r(\mathbf{u}_h^-, \mathbf{u}_h^+)$ is assumed to be a smooth function of the left and right traces of the numerical solution at interface, $\mathbf{u}_h^\mp = \mathbf{u}_h(x^\mp)$ and to be consistent with the physical flux:

$$(2.22) \qquad \boldsymbol{\Phi}_r(\mathbf{u}, \mathbf{u}) = \mathbf{f}(\mathbf{u}) \quad \forall \mathbf{u} \in \mathcal{A}.$$

2.4.2. Space discretization of the adapted problem. Henceforth, each element is associated to a model through a mapping $m : \Omega_h \to \{\text{fine}; \text{equilibrium}\}$. Therefore, the flux function, the source term, and the dimension of the state vector depend on the model $m(\kappa)$ applied to the current cell κ. The numerical flux between two cells with the fine model is $\boldsymbol{\Phi}_r$. At interfaces between two cells with the equilibrium model we use a smooth numerical flux $\boldsymbol{\Phi}_e$ consistent with the physical flux in (2.7):

$$(2.23) \qquad \boldsymbol{\Phi}_e(\mathbf{v}, \mathbf{v}) = \mathbf{f}_v\big(\mathbf{u}_{eq}(\mathbf{v})\big) \quad \forall \mathbf{v} \in \Pi_v \mathcal{A}.$$

The numerical flux between two adjacent cells κ_1 and κ_2 of different kinds, $m(\kappa_1) \neq m(\kappa_2)$, will be defined from the solution of the Riemann problem introduced in subsection 2.2. We split I_h into four different sets (see also Figure 1): $I_h = \gamma_e \cup \gamma_r \cup \gamma_r^e \cup \gamma_e^r$ with

γ_r: set of points between two cells where the fine model is applied;

γ_e: set of points between two cells where the equilibrium model is applied;

γ_r^e: set of points such that the fine model is applied in the left cell and the equilibrium model in the right one;

γ_e^r: set of points such that the equilibrium model is applied in the left cell and the fine model in the right one.

Then, the discrete coupled problem reads find $\mathbf{u}_{hm}$ in V_h such that

$$(2.24) \qquad \mathcal{R}_{hm}(\mathbf{u}_{hm}; \boldsymbol{\psi}_h) = 0 \quad \forall \boldsymbol{\psi}_h \in V_h.$$

Using the domain partition (2.8) and setting $\boldsymbol{\psi}_h = (\boldsymbol{\psi}_h^v, \boldsymbol{\psi}_h^w)^\top$, the space residuals read

(2.25)
$$
\begin{aligned}
\mathcal{R}_{hm}&(\mathbf{u}_{hm}; \boldsymbol{\psi}_h)\\
:=& -\int_{\Omega_r} \mathbf{f}(\mathbf{u}_{hm}) \cdot \partial_x^h \boldsymbol{\psi}_h + \frac{1}{\varepsilon(x)} \mathbf{s}(\mathbf{u}_{hm}) \cdot \boldsymbol{\psi}_h \, dx\\
& -\int_{\Omega_e} \mathbf{f}_v(\mathbf{u}_{eq}(\mathbf{v}_{hm})) \cdot \partial_x^h \boldsymbol{\psi}_h^v + \left(\mathbf{w}_{eq}(\mathbf{v}_{hm}) - \mathbf{w}_{hm}\right) \cdot \boldsymbol{\psi}_h^w \, dx\\
& + \sum_{x \in \gamma_r} \boldsymbol{\Phi}_r(\mathbf{u}_{hm}^-, \mathbf{u}_{hm}^+) \cdot [\![\boldsymbol{\psi}_h]\!]_x + \sum_{x \in \gamma_e} \boldsymbol{\Phi}_e(\mathbf{v}_{hm}^-, \mathbf{v}_{hm}^+) \cdot [\![\boldsymbol{\psi}_h^v]\!]_x\\
& + \sum_{x \in \gamma_r^e} \mathbf{f}\big(\mathcal{W}_r^e(0^-; \mathbf{u}_{hm}^-, \mathbf{v}_{hm}^+)\big) \cdot \boldsymbol{\psi}_h(x^-) - \mathbf{f}_v\big(\mathcal{W}_r^e(0^+; \mathbf{u}_{hm}^-, \mathbf{v}_{hm}^+)\big) \cdot \boldsymbol{\psi}_h^v(x^+)\\
& + \sum_{x \in \gamma_e^r} \mathbf{f}_v\big(\mathcal{W}_e^r(0^-; \mathbf{v}_{hm}^-, \mathbf{u}_{hm}^+)\big) \cdot \boldsymbol{\psi}_h^v(x^-) - \mathbf{f}\big(\mathcal{W}_e^r(0^+; \mathbf{v}_{hm}^-, \mathbf{u}_{hm}^+)\big) \cdot \boldsymbol{\psi}_h(x^+)\\
& - \mathbf{f}\big(\mathcal{W}_r(0^+; \mathbf{b}_0, \mathbf{u}_{hm}(0^+))\big) \cdot \boldsymbol{\psi}_h(0^+) + \mathbf{f}_v\big(\mathcal{W}_e(0^-; \mathbf{v}_{hm}(L^-), \Pi_v \mathbf{b}_L)\big) \cdot \boldsymbol{\psi}_h^v(L^-),
\end{aligned}
$$

where $\mathcal{W}_e(\cdot; \cdot, \cdot)$ stands for the solution of the Riemann problem associated to the equilibrium model in (2.7). Note that the equilibrium state $\mathbf{w} = \mathbf{w}_{eq}(\mathbf{v})$ is imposed weakly in (2.24) (see the second line of (2.25)) and thus will be added as a constraint in the Lagrangian functional for the derivation of error estimators in section 3. This allows the use of the same function space (2.19) for both fine and adapted problems since the vector of degrees of freedom (DOFs) has the same size as in the fine problem in Ω_e with $\mathbf{w}_{hm}$ being the projection of $\mathbf{w}_{eq}(\mathbf{v}_{hm})$ onto the function space (2.19). This technical trick is important, as it allows the derivation of the error representation in section 4.

For the sake of illustration, the fine model is applied in the first cell and the equilibrium model in the last one. We stress that the uniqueness of the solutions to the direct and adjoint problems may depend on boundary conditions and must be considered in each situation.

3. Adjoint problems. We recall the framework of adjoint-based error analysis for target functional in subsection 3.1. Then, we derive the formal adjoint equations to the fine and adapted problems in subsection 3.2 which will be used in section 4 for the derivation of the error estimators.

3.1. Lagrange functionals and assumptions. As indicated in the introduction, we are interested in the rigorous estimation of some Fréchet-differentiable function $J(\mathbf{u})$ of the steady-state solution to problem (2.3)–(2.4). In the following, we

consider functions the form

$$(3.1) \qquad J(\mathbf{u}) = \int_\Omega j(\mathbf{u}, x)\,dx, \quad j(\mathbf{u}, x) = \begin{cases} j(\mathbf{u}) & \text{if } x \in \Omega_r, \\ j(\mathbf{u}_{eq}(\mathbf{v})) & \text{if } x \in \Omega_e, \end{cases}$$

where $j(\cdot)$ is smooth. An example of functional is given in section 6.

J may be estimated from $\mathbf{u}_h$ in V_h the solution to the discrete fine problem (2.20). To lower the cost of the simulation, we are here interested in approximating this function from $\mathbf{u}_{hm}$ in V_h the solution to the discrete adapted problem (2.24) where either the fine or the equilibrium problem is used locally in different regions of the domain Ω. This will be achieved through the use of adaptation algorithms in section 5 based on adjoint a posteriori error bounds derived in section 4.

We underline that it is here customary to assume that the DG function space satisfies $V_h \subset V$ (see, e.g., [24, 26, 16, 25] or [22, section 5]), where V denotes the space that contains the exact primal and dual solutions and will be defined in section 5. We further assume that (2.20) is consistent meaning that $\mathbf{u}$ satisfies

$$(3.2) \qquad \mathcal{R}_h(\mathbf{u}; \boldsymbol{\psi}) = 0 \quad \forall \boldsymbol{\psi} \in V,$$

which requires the consistency of the numerical flux (2.22); see, e.g., [25].

It is useful for the derivation of the error estimates in section 4 to also consider the solution $\mathbf{u}_m$ in V of the formal adapted problem defined by the fine model (2.4) in Ω_r and the equilibrium model (2.6) and (2.7) in Ω_e, together with given boundary and coupling conditions. Likewise, by $\mathbf{z}_m$ we denote the adjoint solution to the adapted problem in strong form, which will be defined in subsection 3.2 by (3.8) in Ω_r, (3.9) in Ω_e, and (3.11) at coupling interfaces, together with adapted boundary conditions from (3.7) and (3.10).

The discrete problem (2.24) is also assumed to be consistent:

$$(3.3) \qquad \mathcal{R}_{hm}(\mathbf{u}_m; \boldsymbol{\psi}) = 0 \quad \forall \boldsymbol{\psi} \in V.$$

We now introduce the following Lagrangian functionals:

$$(3.4a) \qquad \mathscr{L}_h(\mathbf{u}_h; \mathbf{z}_h) := J(\mathbf{u}_h) - \mathcal{R}_h(\mathbf{u}_h; \mathbf{z}_h),$$

$$(3.4b) \qquad \mathscr{L}_{hm}(\mathbf{u}_{hm}; \mathbf{z}_{hm}) := J(\mathbf{u}_{hm}) - \mathcal{R}_{hm}(\mathbf{u}_{hm}; \mathbf{z}_{hm}),$$

where the adjoint variables play the role of Lagrange multipliers associated to the constraints (2.20) and (2.24) [7, 19]. The derivative in the $(\boldsymbol{\varphi}_h, \boldsymbol{\psi}_h)$ direction, for instance, for $\mathscr{L}_h$, reads [36]

$$\begin{aligned} \mathscr{L}'_h\big((\mathbf{u}_h, \mathbf{z}_h); (\boldsymbol{\varphi}_h, \boldsymbol{\psi}_h)\big) &:= \lim_{\theta \to 0^+} \frac{\mathscr{L}_h(\mathbf{u}_h + \theta\boldsymbol{\varphi}_h; \mathbf{z}_h + \theta\boldsymbol{\psi}_h) - \mathscr{L}_h(\mathbf{u}_h; \mathbf{z}_h)}{\theta} \\ &= J'(\mathbf{u}_h; \boldsymbol{\varphi}_h) - \mathcal{R}'_h(\mathbf{u}_h; \boldsymbol{\varphi}_h, \mathbf{z}_h) - \mathcal{R}_h(\mathbf{u}_h; \boldsymbol{\psi}_h). \end{aligned}$$

Stationary points of the Lagrangians in (3.4) correspond to solutions of the associated direct and adjoint problems. The different adjoint problems associated to the function of interest are defined as follows:

$$(3.5a) \qquad \mathbf{z}_h \in V_h : \mathcal{R}'_h(\mathbf{u}_h; \boldsymbol{\varphi}_h, \mathbf{z}_h) = J'(\mathbf{u}_h; \boldsymbol{\varphi}_h) \quad \forall \boldsymbol{\varphi}_h \in V_h,$$

$$(3.5b) \qquad \mathbf{z}_{hm} \in V_h : \mathcal{R}'_{hm}(\mathbf{u}_{hm}; \boldsymbol{\varphi}_h, \mathbf{z}_{hm}) = J'(\mathbf{u}_{hm}; \boldsymbol{\varphi}_h) \quad \forall \boldsymbol{\varphi}_h \in V_h.$$

3.2. Formal adjoint equations. We now derive the formal adjoint equations associated to the fine and adapted problems which will be used in the adjoint consistency analysis in subsection 4.1.

3.2.1. Fine problem. We first assume that the fine model is applied in the full domain: $\Omega_e = \emptyset$ and $\Omega_r = \Omega$. Multiplying the constraint (2.1) at steady state with the Lagrange multiplier $\mathbf{z}$, integrating by parts over Ω, the Lagrangian functional reads

$$\mathscr{L}(\mathbf{u}; \mathbf{z}) = \int_\Omega j(\mathbf{u}) + \mathbf{f}(\mathbf{u})\partial_x \mathbf{z} + \frac{1}{\varepsilon}\mathbf{s}(\mathbf{u})\mathbf{z}\, dx + \mathbf{z}(0^+)\mathbf{f}\big(\mathbf{u}(0^+)\big) - \mathbf{z}(L^-)\mathbf{f}\big(\mathbf{u}(L^-)\big).$$

Linearizing $\mathscr{L}$ about $\mathbf{u}$ in the direction $\boldsymbol{\varphi}$ gives

$$\mathscr{L}'(\mathbf{u}; \boldsymbol{\varphi}, \mathbf{z}) = \int_\Omega \left[j'(\mathbf{u}) + \mathbf{f}'(\mathbf{u})^\top \partial_x \mathbf{z} + \frac{1}{\varepsilon}\mathbf{s}'(\mathbf{u})^\top \mathbf{z} \right] \cdot \boldsymbol{\varphi}\, dx$$
$$+ \left[\mathbf{f}'\big(\mathbf{u}(0^+)\big)^\top \mathbf{z}(0^+) \right] \cdot \boldsymbol{\varphi}(0^+) - \left[\mathbf{f}'\big(\mathbf{u}(L^-)\big)^\top \mathbf{z}(L^-) \right] \cdot \boldsymbol{\varphi}(L^-),$$

which leads to the formal fine adjoint equation

$$(3.6) \qquad \mathbf{f}'(\mathbf{u})^\top \partial_x \mathbf{z} + \frac{1}{\varepsilon(x)}\mathbf{s}'(\mathbf{u})^\top \mathbf{z} = -j'(\mathbf{u}) \quad \text{in } \Omega.$$

Imposing the boundary conditions (2.3) implies formally

$$(3.7)$$
$$\partial_\mathbf{u}\Big(\mathbf{f}\big(\mathcal{W}_r(0^+; \mathbf{b}_0, \mathbf{u}(0^+))\big) \Big)^\top \mathbf{z}(0^+) = 0, \quad \partial_\mathbf{u}\Big(\mathbf{f}\big(\mathcal{W}_r(0^-; \mathbf{u}(L^-), \mathbf{b}_L)\big) \Big)^\top \mathbf{z}(L^-) = 0,$$

where we have used the short notations $\partial_\mathbf{u}(\mathbf{f}(\mathcal{W}(\mathbf{u}))) = \mathbf{f}'(\mathcal{W}(\mathbf{u}))\boldsymbol{\mathcal{W}}'(\mathbf{u})$ for the derivation of composite functions.

Using the notations in (2.5), we rewrite (3.6) as

$$(3.8a) \qquad \partial_\mathbf{v}\mathbf{f}_v^\top \partial_x \mathbf{z}^v + \partial_\mathbf{v}\mathbf{f}_w^\top \partial_x \mathbf{z}^w + \frac{1}{\varepsilon}\mathbf{w}'_{eq}(\mathbf{v})^\top \mathbf{z}^w = -\partial_\mathbf{v} j(\mathbf{u}),$$

$$(3.8b) \qquad \partial_\mathbf{w}\mathbf{f}_v^\top \partial_x \mathbf{z}^v + \partial_\mathbf{w}\mathbf{f}_w^\top \partial_x \mathbf{z}^w - \frac{1}{\varepsilon}\mathbf{z}^w = -\partial_\mathbf{w} j(\mathbf{u}).$$

3.2.2. Adapted problem. Multiplying (3.8b) by $\mathbf{w}'_{eq}(\mathbf{v})^\top$ to the right, summing with (3.8a) to eliminate $\mathbf{z}^w$, and letting $\varepsilon \to 0^+$, one obtains

$$(3.9) \qquad \partial_\mathbf{v}\Big(\mathbf{f}_v\big(\mathbf{u}_{eq}(\mathbf{v})\big) \Big)^\top \partial_x \mathbf{z}^v = -\partial_\mathbf{v}\Big(j\big(\mathbf{u}_{eq}(\mathbf{v})\big) \Big), \quad \mathbf{z}^w = 0,$$

which corresponds to the adjoint equations to the equilibrium model (2.7), thus showing that in the limit $\varepsilon \to 0^+$, the adjoint equations to the fine problem should tend to the adjoint equations to the equilibrium model. This accounts for the choice of same spaces for both fine and adapted adjoint solutions. Likewise, boundary conditions now read

$$(3.10a) \qquad \partial_\mathbf{v}\Big(\mathbf{f}_v\big(\mathbf{u}_{eq}\big(\mathcal{W}_e(0^+; \Pi_v \mathbf{b}_0, \mathbf{v}(0^+))\big)\big) \Big)^\top \mathbf{z}_v(0^+) = 0,$$

$$(3.10b) \qquad \partial_\mathbf{v}\Big(\mathbf{f}_v\big(\mathbf{u}_{eq}\big(\mathcal{W}_e(0^-; \mathbf{v}(L^-), \Pi_v \mathbf{b}_L)\big)\big) \Big)^\top \mathbf{z}_v(L^-) = 0.$$

Finally, the adjoint solution to the adapted problem satisfies the following conditions at coupling interfaces (see notations in subsection 2.4.2):

$$\partial_\mathbf{v}\mathbf{f}\big(\mathbf{u}(x^-)\big)^\top \mathbf{z}(x^-) = \partial_\mathbf{v}\mathbf{f}_v\big(\mathbf{u}_{eq}(\mathbf{v}(x^+))\big)^\top \mathbf{z}^v(x^+), \; \partial_\mathbf{w}\mathbf{f}\big(\mathbf{u}(x^-)\big)^\top \mathbf{z}(x^-)$$
$$(3.11a) \qquad\qquad = 0 \;\; \forall x \in \gamma_r^e,$$

$$\partial_\mathbf{v}\mathbf{f}_v\big(\mathbf{u}_{eq}(\mathbf{v}(x^-))\big)^\top \mathbf{z}^v(x^-) = \partial_\mathbf{v}\mathbf{f}\big(\mathbf{u}(x^+)\big)^\top \mathbf{z}(x^+), \; \partial_\mathbf{w}\mathbf{f}\big(\mathbf{u}(x^+)\big)^\top \mathbf{z}(x^+)$$
$$(3.11b) \qquad\qquad = 0 \;\; \forall x \in \gamma_e^r,$$

where specific coupling conditions have to be included together with specific boundary conditions at the domain boundaries.

Example 1 (Jin–Xin relaxation). Here, we revisit the example (2.14)–(2.17) of the adapted problem based on the Jin–Xin relaxation system and its equilibrium scalar equation. Using the above procedure, the formal adjoint equations to the steady-state problem read

(3.12)
$$
\begin{cases}
\begin{cases}
\partial_x z^v - \frac{1}{\varepsilon} z^w = -\partial_w j(v, w), & x \in \Omega_r, \\
a^2 \partial_x z^w + \frac{1}{\varepsilon} f'(v) z^w = -\partial_v j(v, w),
\end{cases} \\
\begin{cases}
f'(v)\partial_x z^v = -\partial_v j\big(v, w_{eq}(v)\big), & x \in \Omega_e, \\
z^w = 0,
\end{cases}
\end{cases}
$$

together with the boundary condition at $x = 0$ and coupling conditions at x_c in γ_r^e,

(3.13)
$$
z^v(0^+) = 0, \quad f'\big(v(x_c^+)\big)\big(z^v(x_c^-) - z^v(x_c^+)\big) = 0, \quad z^w(x_c^-) = 0,
$$

which impose continuity of the adjoint solution at the coupling interface when $f'(v(x_c^+))$ is nonzero and may be compared to the interior boundary condition at noncharacteristic stationary shocks [18].

4. Representation of the modeling and discretization errors. In subsection 4.1, we first prove adjoint consistency of the fine and adapated adjoint problems. These results are then used in subsection 4.2 for the derivation of adjoint-based representations of the error $J(\mathbf{u}) - J(\mathbf{u}_{hm})$ on a given functional. The main result is Theorem 5, which provides local a posteriori estimators of both modeling and discretization errors.

4.1. Adjoint consistency analysis. Lemma 1 states the adjoint consistency of the discrete fine problem, while Lemma 2 states consistency of the discrete adapted problem. An illustration for Lemma 2 is then given in Example 2.

LEMMA 1. *Assume that the numerical flux $\mathbf{\Phi}_r$ is consistent, (2.22), and differentiable. Then, the discrete fine adjoint problem (3.5a) is consistent with the continuous fine adjoint problem:*

(4.1)
$$
\mathcal{R}'_h(\mathbf{u}; \boldsymbol{\varphi}, \mathbf{z}) = J'(\mathbf{u}; \boldsymbol{\varphi}) \quad \forall \boldsymbol{\varphi} \in V.
$$

Proof. The derivative of the discrete residual (2.21) reads

$$
\begin{aligned}
\mathcal{R}'_h(\mathbf{u}; \boldsymbol{\varphi}, \mathbf{z}) := & -\int_{\Omega_h} [\mathbf{f}'(\mathbf{u})\boldsymbol{\varphi}] \cdot \partial_x^h \mathbf{z} + \frac{1}{\varepsilon}[\mathbf{s}'(\mathbf{u})\boldsymbol{\varphi}] \cdot \mathbf{z} \, dx \\
& + \sum_{x \in I_h} \big[\partial_1 \mathbf{\Phi}_r(\mathbf{u}^-, \mathbf{u}^+)\boldsymbol{\varphi}^- + \partial_2 \mathbf{\Phi}_r(\mathbf{u}^-, \mathbf{u}^+)\boldsymbol{\varphi}^+\big] \cdot [\![\mathbf{z}]\!]_x \\
& + \Big[\partial_{\mathbf{u}}\Big(\mathbf{f}\big(\mathcal{W}_r(0^+; \mathbf{b}_0, \mathbf{u}(0^+))\big)\Big)\boldsymbol{\varphi}(0^+)\Big] \cdot \mathbf{z}(0^+) \\
& - \Big[\partial_{\mathbf{u}}\Big(\mathbf{f}\big(\mathcal{W}_r(0^-; \mathbf{u}(L^-), \mathbf{b}_L)\big)\Big)\boldsymbol{\varphi}(L^-)\Big] \cdot \mathbf{z}(L^-),
\end{aligned}
$$

where ∂_1 and ∂_2 denote the partial derivatives with respect to the first and second arguments, respectively. By regularity of the adjoint variable, we get $[\![\mathbf{z}]\!]_x = 0$. Then,

using (3.6) and (3.7) we obtain

$$\mathcal{R}'_h(\mathbf{u}; \boldsymbol{\varphi}, \mathbf{z}) = \int_\Omega j'(\mathbf{u}) \cdot \boldsymbol{\varphi} \, dx = J'(\mathbf{u}; \boldsymbol{\varphi}),$$

which completes the proof.   □

LEMMA 2. *Assume that the numerical fluxes* $\boldsymbol{\Phi}_r$ *and* $\boldsymbol{\Phi}_e$ *are consistent and differentiable,* (2.22) *and* (2.23)*, and that the coupling numerical flux is consistent and differentiable,* (2.11)*; then the discrete adapted adjoint problem* (2.24) *and* (2.25) *is consistent with the continuous adapted adjoint problem* (3.5b)*:*

(4.2) $$\mathcal{R}'_{hm}(\mathbf{u}_m; \boldsymbol{\varphi}, \mathbf{z}_m) = J'(\mathbf{u}_m; \boldsymbol{\varphi}) \quad \forall \boldsymbol{\varphi} \in V.$$

Proof. The adjoint consistency in the fine domain has been proved in Lemma 1, and the adjoint consistency in the equilibrium domain relies on the same techniques. It remains to show that the contributions from the coupling interfaces vanish. Let

$$\mathcal{C}^e_r(\mathbf{u}_{hm}; \boldsymbol{\psi}_h) := \sum_{x \in \gamma^e_r} \mathbf{f}\big(\mathcal{W}^e_r(0^-; \mathbf{u}^-_{hm}, \mathbf{v}^+_{hm})\big) \cdot \boldsymbol{\psi}_h(x^-) - \mathbf{f}_v\big(\mathcal{W}^e_r(0^+; \mathbf{u}^-_{hm}, \mathbf{v}^+_{hm})\big) \cdot \boldsymbol{\psi}^v_h(x^+)$$

be the contributions from interfaces γ^e_r to (2.25). Its counterpart $\mathcal{C}^r_e$ from interfaces in γ^r_e is defined in a similar way and leads to the same conclusion. Linearizing the above terms, we get

$$
\begin{aligned}
\mathcal{C}^{e'}_r(\mathbf{u}_{hm}; \boldsymbol{\varphi}_h, \mathbf{z}_{hm}) &= \sum_{x \in \gamma^e_r} \Big[\partial_{\mathbf{u}}\Big(\mathbf{f}\big(\mathcal{W}^e_r(0^-; \mathbf{u}^-_{hm}, \mathbf{v}^+_{hm})\big)\Big) \boldsymbol{\varphi}_h(x^-) \Big] \cdot \mathbf{z}_{hm}(x^-) \\
&\quad - \Big[\partial_{\mathbf{v}}\Big(\mathbf{f}_v\big(\mathcal{W}^e_r(0^+; \mathbf{u}^-_{hm}, \mathbf{v}^+_{hm})\big)\Big) \boldsymbol{\varphi}^v_h(x^+) \Big] \cdot \mathbf{z}^v_{hm}(x^+) \\
&= \sum_{x \in \gamma^e_r} \boldsymbol{\varphi}_h(x^-)^\top \partial_{\mathbf{u}}\Big(\mathbf{f}\big(\mathcal{W}^e_r(0^-; \mathbf{u}^-_{hm}, \mathbf{v}^+_{hm})\big)\Big)^\top \mathbf{z}_{hm}(x^-) \\
&\quad - \boldsymbol{\varphi}^v_h(x^+)^\top \partial_{\mathbf{v}}\Big(\mathbf{f}_v\big(\mathcal{W}^e_r(0^+; \mathbf{u}^-_{hm}, \mathbf{v}^+_{hm})\big)\Big)^\top \mathbf{z}^v_{hm}(x^+) \\
&= \sum_{x \in \gamma^e_r} \boldsymbol{\varphi}^v_h(x^-)^\top \partial_{\mathbf{v}}\Big(\mathbf{f}\big(\mathcal{W}^e_r(0^-; \mathbf{u}^-_{hm}, \mathbf{v}^+_{hm})\big)\Big)^\top \mathbf{z}_{hm}(x^-) \\
&\quad + \boldsymbol{\varphi}^w_h(x^-)^\top \partial_{\mathbf{w}}\Big(\mathbf{f}\big(\mathcal{W}^e_r(0^-; \mathbf{u}^-_{hm}, \mathbf{v}^+_{hm})\big)\Big)^\top \mathbf{z}_{hm}(x^-) \\
&\quad - \boldsymbol{\varphi}^v_h(x^+)^\top \partial_{\mathbf{v}}\Big(\mathbf{f}_v\big(\mathcal{W}^e_r(0^+; \mathbf{u}^-_{hm}, \mathbf{v}^+_{hm})\big)\Big)^\top \mathbf{z}^v_{hm}(x^+),
\end{aligned}
$$

where the two last steps follow from manipulations of matrix-vector products. Substituting the exact direct and adjoint solutions and using consistency of the Riemann problem (2.11), we get

$$
\begin{aligned}
\mathcal{C}^{e'}_r(\mathbf{u}_m; \boldsymbol{\varphi}, \mathbf{z}_m) &= \sum_{x \in \gamma^e_r} \Big(\boldsymbol{\varphi}^v(x^-)^\top \partial_{\mathbf{v}}\mathbf{f}\big(\mathbf{u}(0^-)\big)^\top + \boldsymbol{\varphi}^w(x^-)^\top \partial_{\mathbf{w}}\mathbf{f}\big(\mathbf{u}(0^-)\big)^\top \Big) \mathbf{z}_m(x^-) \\
&\quad - \boldsymbol{\varphi}^v(x^+)^\top \partial_{\mathbf{v}}\mathbf{f}_v\big(\mathbf{u}_{eq}(\mathbf{v}(0^+))\big)^\top \cdot \mathbf{z}^v_m(x^+),
\end{aligned}
$$

which indeed vanishes from (3.11a).   □

Example 2 (Jin–Xin relaxation). We consider the discretization (2.25) of the Jin–Xin problem (2.14)–(2.17):

$$
\begin{aligned}
&\mathcal{R}_{hm}(\mathbf{u}_{hm}; \boldsymbol{\psi}_h) \\
&= -\int_0^{x_c} \mathbf{f}(\mathbf{u}_{hm}) \cdot \partial_x^h \boldsymbol{\psi}_h + \tfrac{1}{\varepsilon}(f(v_{hm}) - w_{hm})\psi_h^w \, dx + \sum_{x \in \gamma_r} \boldsymbol{\Phi}_r(\mathbf{u}_{hm}^-, \mathbf{u}_{hm}^+) \cdot [\![\boldsymbol{\psi}_h]\!]_x \\
&\quad - \int_{x_c}^L f(v_{hm})\partial_x^h \psi_h^v + \big(f(v_{hm}) - w_{hm}\big)\psi_h^w \, dx + \sum_{x \in \gamma_e} \Phi_e(v_{hm}^-, v_{hm}^+)[\![\psi_h^v]\!]_x \\
&\quad + f\big(v_{hm}(x_c^+)\big)\psi_h^v(x_c^-) + a^2 v_{hm}(x_c^-)\psi_h^w(x_c^-) - f\big(v_{hm}(x_c^+)\big)\psi_h^v(x_c^+) \\
&\quad - w_{hm}(0^+)\psi_h^v(0^+) - a^2 b_0 \psi_h^w(0^+) + f(b_L)\psi_h^v(L^-),
\end{aligned}
$$

where $\mathbf{u}_{hm}(x_c^\pm) = \mathcal{W}_r^e(0^\pm; \mathbf{u}_{hm}^-, v_{hm}^+)$, and we have applied the first condition in (2.15) and the boundary conditions (2.17). Using the above procedures, it may be easily shown that the above discretization is differentiable, consistent, and adjoint consistent.

4.2. A posteriori error analysis. Let us consider the two errors:

$$
(4.3) \qquad\qquad \boldsymbol{\epsilon}_{hm} := \mathbf{u} - \mathbf{u}_{hm}, \qquad \boldsymbol{e}_m := \mathbf{z} - \mathbf{z}_m,
$$

which correspond to the error on the solution to the discrete direct adapted problem and the model error on the solution to the adjoint problem, respectively.

In Theorem 5, we establish the representation of the discretization and model errors on the function of interest. This estimate is based on Lemmas 3 and 4, also derived in previous works [9, 36], which provide estimators that are third-order and second-order accurate in $\boldsymbol{\epsilon}_{hm}$, respectively, but require the computation of $\mathbf{z}$ the formal adjoint solution to the fine problem. Theorem 5 is a quadratic error estimate in $\boldsymbol{e}_m$ and $\boldsymbol{\epsilon}_{hm}$ that only involves $\mathbf{z}_m$ the formal adjoint solution to the adapted problem.

LEMMA 3. *Let* $\mathbf{u}$ *and* $\mathbf{z}$ *in* V *be the solutions to the continuous fine direct and adjoint problems, respectively. Then, under the assumptions of Lemma 2 the solution* $\mathbf{u}_{hm}$ *to* (2.24) *satisfies*
$$
(4.4)
$$
$$
J(\mathbf{u}) - J(\mathbf{u}_{hm}) = -\mathcal{R}_h(\mathbf{u}_{hm}; \boldsymbol{\psi}_h) + \frac{1}{2}\mathcal{L}_h'\big((\mathbf{u}_{hm}; \boldsymbol{\psi}_h); (\boldsymbol{\epsilon}_{hm}, \mathbf{z} - \boldsymbol{\psi}_h)\big) + \mathcal{O}(\|\boldsymbol{\epsilon}_{hm}\|_V^3),
$$

for all $\boldsymbol{\psi}_h$ *in* V_h *with* $\|\cdot\|_V$ *a norm on* V *and*
$$
(4.5)
$$
$$
\mathcal{L}_h'\big((\mathbf{u}_{hm}; \boldsymbol{\psi}_h); (\boldsymbol{\epsilon}_{hm}, \mathbf{z} - \boldsymbol{\psi}_h)\big) = J'(\mathbf{u}_{hm}; \boldsymbol{\epsilon}_{hm}) - \mathcal{R}_h'(\mathbf{u}_{hm}; \boldsymbol{\epsilon}_{hm}, \boldsymbol{\psi}_h) - \mathcal{R}_h(\mathbf{u}_{hm}, \mathbf{z} - \boldsymbol{\psi}_h).
$$

Proof. Let $\boldsymbol{\psi}_h$ in V_h; from (3.2) we get

$$
\begin{aligned}
J(\mathbf{u}) - J(\mathbf{u}_{hm}) &= J(\mathbf{u}) - J(\mathbf{u}_{hm}) - \mathcal{R}_h(\mathbf{u}; \mathbf{z}) \\
&= J(\mathbf{u}) - \mathcal{R}_h(\mathbf{u}; \mathbf{z}) - J(\mathbf{u}_{hm}) + \mathcal{R}_h(\mathbf{u}_{hm}; \boldsymbol{\psi}_h) - \mathcal{R}_h(\mathbf{u}_{hm}; \boldsymbol{\psi}_h) \\
&= \mathcal{L}_h(\mathbf{u}; \mathbf{z}) - \mathcal{L}_h(\mathbf{u}_{hm}; \boldsymbol{\psi}_h) - \mathcal{R}_h(\mathbf{u}_{hm}; \boldsymbol{\psi}_h).
\end{aligned}
$$

Then, using the trapezoidal rule gives

$$
\begin{aligned}
&\mathcal{L}_h(\mathbf{u}; \mathbf{z}) - \mathcal{L}_h(\mathbf{u}_{hm}; \boldsymbol{\psi}_h) \\
&= \mathcal{L}_h(\mathbf{u}_{hm} + \boldsymbol{\epsilon}_{hm}; \boldsymbol{\psi}_h + \mathbf{z} - \boldsymbol{\psi}_h) - \mathcal{L}_h(\mathbf{u}_{hm}; \boldsymbol{\psi}_h) \\
&= \frac{1}{2}\Big[\mathcal{L}_h'\big((\mathbf{u}; \mathbf{z}); (\boldsymbol{\epsilon}_{hm}, \mathbf{z} - \boldsymbol{\psi}_h)\big) + \mathcal{L}_h'\big((\mathbf{u}_{hm}; \boldsymbol{\psi}_h); (\boldsymbol{\epsilon}_{hm}, \mathbf{z} - \boldsymbol{\psi}_h)\big)\Big] \\
&\quad + \int_0^1 \mathcal{L}'''\big([\mathbf{u}_{hm} + s\,\boldsymbol{\epsilon}_{hm}, \boldsymbol{\psi}_h + s\,(\mathbf{z} - \boldsymbol{\psi}_h)]; \hat{\boldsymbol{r}}, \hat{\boldsymbol{r}}, \hat{\boldsymbol{r}}\big)s(1 - s)\,ds,
\end{aligned}
$$

where $\hat{r} = (\boldsymbol{\epsilon}_{hm}, \mathbf{z} - \boldsymbol{\psi}_h)$. Using consistency of the direct and adjoint problems, (3.2) and (4.1), together with $V_h \subset V$, we get

$$\mathscr{L}'_h((\mathbf{u}; \mathbf{z}); (\boldsymbol{\epsilon}_{hm}, \mathbf{z} - \boldsymbol{\psi}_h)) = J'(\mathbf{u}; \boldsymbol{\epsilon}_{hm}) - \mathcal{R}'_h(\mathbf{u}; \boldsymbol{\epsilon}_{hm}, \mathbf{z}) - \mathcal{R}_h(\mathbf{u}; \mathbf{z} - \boldsymbol{\psi}_h) = 0,$$

which completes the proof. □

LEMMA 4. *Let* $\mathbf{u}$ *and* $\mathbf{z}$ *in* V *be the solutions to the continuous fine direct and adjoint problems, respectively. Then, under the assumptions of Lemma 2 the solution* $\mathbf{u}_{hm}$ *to* (2.24) *satisfies*

$$(4.6) \qquad J(\mathbf{u}) - J(\mathbf{u}_{hm}) = -\mathcal{R}_h(\mathbf{u}_{hm}, \mathbf{z}) + \mathcal{O}(\|\boldsymbol{\epsilon}_{hm}\|_V^2).$$

Proof. Let $\boldsymbol{\psi}_h \in V_h$; by consistency of the direct problem (3.2), the last term in (4.5) reads

$$\begin{aligned}
\mathcal{R}_h(\mathbf{u}_{hm}; \mathbf{z} - \boldsymbol{\psi}_h) &= \mathcal{R}_h(\mathbf{u}_{hm}; \mathbf{z} - \boldsymbol{\psi}_h) - \mathcal{R}_h(\mathbf{u}; \mathbf{z} - \boldsymbol{\psi}_h) \\
&= -\big(\mathcal{R}_h(\mathbf{u}_{hm} + \boldsymbol{\epsilon}_{hm}; \mathbf{z} - \boldsymbol{\psi}_h) - \mathcal{R}_h(\mathbf{u}_{hm}; \mathbf{z} - \boldsymbol{\psi}_h)\big) \\
(4.7) \qquad &= -\mathcal{R}'_h(\mathbf{u}_{hm}; \boldsymbol{\epsilon}_{hm}, \mathbf{z} - \boldsymbol{\psi}_h) - \Delta R_1,
\end{aligned}$$

where we have applied the midpoint rule in the last step with

$$\Delta R_1 = \int_0^1 \mathcal{R}''_h(\mathbf{u}_{hm} + s\,\boldsymbol{\epsilon}_{hm}; \boldsymbol{\epsilon}_{hm}, \boldsymbol{\epsilon}_{hm}, \mathbf{z} - \boldsymbol{\psi}_h)(1 - s)\, ds.$$

Again, by consistency (4.1) the two first terms in the right-hand side of (4.5) become

$$\begin{aligned}
J'(\mathbf{u}_{hm}; \boldsymbol{\epsilon}_{hm}) - \mathcal{R}'_h(\mathbf{u}_{hm}; \boldsymbol{\epsilon}_{hm}, \boldsymbol{\psi}_h) =& J'(\mathbf{u}_{hm}; \boldsymbol{\epsilon}_{hm}) - \mathcal{R}'_h(\mathbf{u}_{hm}; \boldsymbol{\epsilon}_{hm}, \boldsymbol{\psi}_h) \\
& - \big(J'(\mathbf{u}; \boldsymbol{\epsilon}_{hm}) - \mathcal{R}'_h(\mathbf{u}; \boldsymbol{\epsilon}_{hm}, \mathbf{z})\big) \\
=& - \big(J'(\mathbf{u}_{hm} + \boldsymbol{\epsilon}_{hm}; \boldsymbol{\epsilon}_{hm}) - J'(\mathbf{u}_{hm}; \boldsymbol{\epsilon}_{hm})\big) \\
& + \mathcal{R}'_h(\mathbf{u}_{hm}; \boldsymbol{\epsilon}_{hm}, \mathbf{z} - \boldsymbol{\psi}_h) \\
& + \mathcal{R}'_h(\mathbf{u}_{hm} + \boldsymbol{\epsilon}_{hm}; \boldsymbol{\epsilon}_{hm}, \mathbf{z}) - \mathcal{R}'_h(\mathbf{u}_{hm}; \boldsymbol{\epsilon}_{hm}, \mathbf{z}) \\
=& - \Delta J + \mathcal{R}'_h(\mathbf{u}_{hm}; \boldsymbol{\epsilon}_{hm}, \mathbf{z} - \boldsymbol{\psi}_h) + \Delta R_2,
\end{aligned}$$

where

$$\Delta J = \int_0^1 J''(\mathbf{u}_{hm} + s\boldsymbol{\epsilon}_{hm}; \boldsymbol{\epsilon}_{hm}, \boldsymbol{\epsilon}_{hm})\, ds, \quad \Delta R_2 = \int_0^1 \mathcal{R}''_h(\mathbf{u}_{hm} + s\boldsymbol{\epsilon}_{hm}; \boldsymbol{\epsilon}_{hm}, \boldsymbol{\epsilon}_{hm}, \mathbf{z})\, ds.$$

We use the above results to evaluate (4.5),

$$\begin{aligned}
\mathscr{L}'_h\big((\mathbf{u}_{hm}; \boldsymbol{\psi}_h); (\boldsymbol{\epsilon}_{hm}, \mathbf{z} - \boldsymbol{\psi}_h)\big) &= 2\mathcal{R}'_h(\mathbf{u}_{hm}; \boldsymbol{\epsilon}_{hm}, \mathbf{z} - \boldsymbol{\psi}_h) + \Delta R_2 + \Delta R_1 - \Delta J \\
&= -2\mathcal{R}_h(\mathbf{u}_{hm}; \mathbf{z} - \boldsymbol{\psi}_h) + \Delta R_2 - \Delta R_1 - \Delta J,
\end{aligned}$$

from (4.7), and conclude by inserting the result into the estimate (4.4) in Lemma 3. □

THEOREM 5. *Let* $\mathbf{u}$ *in* V *be the solution to the continuous direct fine problem and* $\mathbf{z}_m$ *in* V *the solution of the continuous adjoint adapted problem. Then, under the assumptions of Lemma 2 the solution* $\mathbf{u}_{hm}$ *to* (2.24) *satisfies*

$$\begin{aligned}
(4.8a) \qquad J(\mathbf{u}) - J(\mathbf{u}_{hm}) &= - \mathcal{R}_h(\mathbf{u}_{hm}; \mathbf{z}_m) + \mathcal{O}(\|\boldsymbol{\epsilon}_{hm}\|_V \|\mathbf{e}_m\|_V, \|\boldsymbol{\epsilon}_{hm}\|_V^2), \\
(4.8b) \qquad &\simeq - \mathcal{R}_h(\mathbf{u}_{hm}; \boldsymbol{\psi}_h) - \mathcal{R}_h(\mathbf{u}_{hm}; \mathbf{z}_m - \boldsymbol{\psi}_h) \quad \forall \boldsymbol{\psi}_h \in V_h.
\end{aligned}$$

Proof. We start from the previous estimate (4.6) and the definitions of the errors (4.3). Using the consistency of the direct problem (3.2), we get

$$
\begin{aligned}
\mathcal{R}_h(\mathbf{u}_{hm}; \mathbf{z}) &= \mathcal{R}_h(\mathbf{u}_{hm}; \mathbf{z}_m) + \mathcal{R}_h(\mathbf{u}_{hm}; \boldsymbol{e}_m) \\
&= \mathcal{R}_h(\mathbf{u}_{hm}; \mathbf{z}_m) + \mathcal{R}_h(\mathbf{u}_{hm}; \boldsymbol{e}_m) - \mathcal{R}_h(\mathbf{u}; \boldsymbol{e}_m) \\
&= \mathcal{R}_h(\mathbf{u}_{hm}; \mathbf{z}_m) + \mathcal{R}_h(\mathbf{u}_{hm}; \boldsymbol{e}_m) - \mathcal{R}_h(\mathbf{u}_{hm} + \boldsymbol{\epsilon}_{hm}; \boldsymbol{e}_m) \\
&= \mathcal{R}_h(\mathbf{u}_{hm}; \mathbf{z}_m) - \int_0^1 \mathcal{R}'_h(\mathbf{u}_{hm} + s\,\boldsymbol{\epsilon}_{hm}; \boldsymbol{\epsilon}_{hm}, \boldsymbol{e}_m)\, ds,
\end{aligned}
$$

and we conclude by linearity of $\mathcal{R}_h(\mathbf{u}_{hm}; \cdot)$.   □

4.3. Comments on Theorem 5. The estimate (4.8) only requires the continuous adjoint solution to the adapted problem, and we will use usual arguments for its approximation in section 5. The first term in (4.8b) represents the model error and has no contributions in regions where the fine solution is used, while the second term represents the discretization error. Indeed, assume first that we consider the fine model only, $\mathbf{u}_{hm} = \mathbf{u}_h$ and $\mathbf{z}_m = \mathbf{z}$; then by consistency (4.8) becomes

$$
(4.9) \qquad\qquad J(\mathbf{u}) - J(\mathbf{u}_h) \simeq -\mathcal{R}_h(\mathbf{u}_h; \mathbf{z} - \boldsymbol{\psi}_h),
$$

which constitutes the usual adjoint-based discretization error representation [7, 24]. Now, assume that we consider only modeling approximation $\mathbf{u}_{hm} = \mathbf{u}_m$; (4.8) becomes

$$
J(\mathbf{u}) - J(\mathbf{u}_m) \simeq -\mathcal{R}_h(\mathbf{u}_m; \mathbf{z}_m) = -\big(\mathcal{R}_h(\mathbf{u}_m; \mathbf{z}_m) - \mathcal{R}_{hm}(\mathbf{u}_m; \mathbf{z}_m)\big),
$$

from (3.3), which constitutes the equivalent of the adjoint-based model error representation in [9] for hyperbolic systems with relaxation.

Finally, note that the error representation in Theorem 5 is second-order accurate only if the discretization and model errors are balanced, which will constitute the aim of the adaptation algorithm described in section 5.

5. *hpm*-adaptation. In this section, we describe the adaptation algorithm based on the error representation (4.8) derived in the previous section. The error representation involves $\mathbf{z}_m$ in V the adjoint solution to the continuous adapted problem and is based on the assumption $V_h \subset V$. The solution $\mathbf{z}_m$ is usually approximated by $\hat{\mathbf{z}}_{hm}$ in a discrete space $\hat{V}_h \supset V_h$ obtained by subdividing the mesh or increasing the local polynomial degree of the numerical solution [24]:

$$
(5.1) \qquad\qquad \mathcal{R}'_{hm}(\mathbf{u}_{hm}; \boldsymbol{\varphi}_h, \hat{\mathbf{z}}_{hm}) = J'(\mathbf{u}_{hm}; \boldsymbol{\varphi}_h) \quad \forall \boldsymbol{\varphi}_h \in \hat{V}_h.
$$

Substituting $\mathbf{z}_m$ for $\hat{\mathbf{z}}_{hm}$ into (4.8) and using a triangle inequality, we introduce the local error estimators as follows:

$$
(5.2) \qquad\quad |J(\mathbf{u}) - J(\mathbf{u}_{hm})| \lesssim \sum_{\kappa \in \Omega_h} \eta_\kappa^h\big(\mathbf{u}_{hm}; \hat{\mathbf{z}}_{hm}\big) + \eta_\kappa^m\big(\mathbf{u}_{hm}; \hat{\mathbf{z}}_{hm}\big),
$$

where η_κ^h and η_κ^m are the elementwise discretization and modeling error estimators, respectively. Setting $\boldsymbol{\psi}_h = \pi_h \hat{\mathbf{z}}_{hm}$ into (4.8) with $\pi_h : \hat{V}_h \to V_h$ the orthogonal projector onto V_h, we have
(5.3)
$$
\eta_\kappa^h\big(\mathbf{u}_{hm}; \hat{\mathbf{z}}_{hm}\big) = |\mathcal{R}_h(\mathbf{u}_{hm}; 1_\kappa(\hat{\mathbf{z}}_{hm} - \pi_h \hat{\mathbf{z}}_{hm}))|, \quad \eta_\kappa^m\big(\mathbf{u}_{hm}; \hat{\mathbf{z}}_{hm}\big) = |\mathcal{R}_h(\mathbf{u}_{hm}; 1_\kappa \pi_h \hat{\mathbf{z}}_{hm})|,
$$

where 1_κ denotes the indicator function of κ.

Remark 6. Though η_κ^h relies on usual techniques [7, 24], η_κ^m is not standard. Let $\kappa = (a, b)$ in Ω_h, and consider the following situations for the sake of illustration:
- if $\kappa \in \Omega_r$, $\partial\kappa \cap \gamma_e^r = \partial\kappa \cap \gamma_r^e = \emptyset$, then the fine model is applied so

$$\eta_\kappa^m\big(\mathbf{u}_{hm}; \hat{\mathbf{z}}_{hm}\big) = 0;$$

- if $\kappa \in \Omega_e$, $\partial\kappa \cap \gamma_e^r = \partial\kappa \cap \gamma_r^e = \emptyset$, then $\mathbf{u}_{hm} = \mathbf{u}_{eq}(\mathbf{v}_{hm})$ and

$$\eta_\kappa^m\big(\mathbf{u}_{hm}; \hat{\mathbf{z}}_{hm}\big) = -\int_\kappa \mathbf{f}_w(\mathbf{u}_{hm}) \cdot d_x\hat{\mathbf{z}}_{hm}^w dx + \big[\boldsymbol{\Phi}_r^w(\mathbf{u}_{hm}^-, \mathbf{u}_{hm}^+) \cdot \hat{\mathbf{z}}_{hm}^w\big]_{x=a^+}^{x=b^-};$$

- if $\kappa \in \Omega_r$, $b \in \gamma_r^e$, and $\partial\kappa \cap \gamma_e^r = \emptyset$, then $\mathbf{u}_{hm}(b^+) = \mathbf{u}_{eq}(\mathbf{v}_{hm}(b^+))$ and

$$\eta_\kappa^m\big(\mathbf{u}_{hm}; \hat{\mathbf{z}}_{hm}\big) = \Big(\boldsymbol{\Phi}_r(\mathbf{u}_{hm}^-, \mathbf{u}_{hm}^+) - \mathbf{f}\big(\mathcal{W}_r^e(0^-; \mathbf{u}_{hm}^-, \mathbf{v}_{hm}^+)\big)\Big)_{x=b} \cdot \hat{\mathbf{z}}_{hm}(b^-);$$

- if $\kappa \in \Omega_e$, $a \in \gamma_r^e$, and $\partial\kappa \cap \gamma_e^r = \emptyset$, then $\mathbf{u}_{hm}(a^+) = \mathbf{u}_{eq}(\mathbf{v}_{hm}(a^+))$ and

$$\begin{aligned}
\eta_\kappa^m\big(\mathbf{u}_{hm}; \hat{\mathbf{z}}_{hm}\big) = &-\int_\kappa \mathbf{f}_w(\mathbf{u}_{hm}) \cdot d_x\hat{\mathbf{z}}_{hm}^w dx + \boldsymbol{\Phi}_r^w\big(\mathbf{u}_{hm}(b^-), \mathbf{u}_{hm}(b^+)\big) \cdot \hat{\mathbf{z}}_{hm}^w(b^-) \\
&- \boldsymbol{\Phi}_r\big(\mathbf{u}_{hm}(a^-), \mathbf{u}_{hm}(a^+)\big) \cdot \hat{\mathbf{z}}_{hm}(a^+) \\
&+ \mathbf{f}_v\big(\mathcal{W}_r^e(0^+; \mathbf{u}_{hm}^-, \mathbf{v}_{hm}^+)\big)_{x=a} \cdot \hat{\mathbf{z}}_{hm}^v(a^+).
\end{aligned}$$

The refinement algorithm is based on the local estimators (5.3). We start with an initial mesh Ω_h, an initial degree function $p : \Omega_h \to \mathbb{N}$, and a model map $m : \Omega_h \to \{\text{fine; equilibrium}\}$. Algorithm 1 describes the main steps of the adaptation process. The main loop 3 aims at driving the error in J to the required tolerance (1.1). This is achieved by locally adapting the mesh, the polynomial degree, and the model through Algorithm 2.

Algorithm 1 *hpm*-adaptation.

1: Set `ERR` $\gg 1$
2: $\forall \kappa \in \Omega_h$, $\eta_\kappa^m \leftarrow 0$, $\eta_\kappa^h \leftarrow 0$
3: **while** `ERR` $>$ `TOL` $\times J(\mathbf{u}_{hm})$ **do**
4:     compute $\mathbf{u}_{hm}$ from (2.24) and $\hat{\mathbf{z}}_{hm}$ from (5.1)
5:     compute `ERR` $= \sum_{\kappa \in \Omega_h} \eta_\kappa^m\big(\mathbf{u}_{hm}; \hat{\mathbf{z}}_{hm}\big) + \eta_\kappa^h\big(\mathbf{u}_{hm}; \hat{\mathbf{z}}_{hm}\big)$ from (5.3)
6:     adapt V_h with Algorithm 2
7: **end while**
8: **return** $\mathbf{u}_{hm}$ and $J(\mathbf{u}_{hm})$

The adaptation procedure in Algorithm 2 consists in refining a fixed fraction of the total number of mesh elements and constitutes a very crude algorithm that may be replaced by any other more sophisticated technique. The present work rather focuses on the reliability and sharpness of the error estimators in the context of *hpm*-adaptation of hyperbolic systems with relaxation. Local discretization and model errors are first compared, which allows to select the refinement process so as to balance both error components. In the case of a discretization refinement, either the polynomial degree is increased or the mesh is subdivided according to the local smoothness of the solution. In this work, the smoothness of $\mathbf{u}_m$ is evaluated through the decay of the coefficients of its approximation $\mathbf{u}_{hm}$ in the basis of Legendre polynomials. In the case of a model refinement, the sets of coupling interfaces γ_r^e and γ_e^r separating different models in the space residuals (2.25) are updated before a new cycle.

Algorithm 2 adapt V_h.

1: Set $\Omega_h^{ref} \subset \Omega_h$ with largest estimators $\eta_\kappa^h + \eta_\kappa^m$
2: **for** $\kappa \in \Omega_h^{ref}$ **do**
3:     **if** $\eta_\kappa^h > \eta_\kappa^m$ **then**
4:         **if** $\mathbf{u}_{hm}$ is smooth on κ **then**
5:             $p(\kappa) \leftarrow p(\kappa) + 1$
6:         **else**
7:            split κ into two cells
8:         **end if**
9:     **else**
10:         $m(\kappa) \leftarrow$ fine
11:     **end if**
12: **end for**

---

6. Numerical experiments. In this section, we perform some numerical simulations of the Jin–Xin model (2.12). The Rusanov flux is used as numerical flux at internal faces. We apply the adaptation procedure introduced in section 5 with different physical fluxes f and based on the error estimators (5.2) and (5.3). For all the simulations, we aim at evaluating the functional (3.1) with $j(\mathbf{u}) = \frac{1}{2}(v - b_L)^2$ and a tolerance TOL $= 10^{-12}$ in (1.1). The efficiency of the present method is compared to results from an hp-adaptation algorithm with local error estimators derived from (4.9). Starting from a uniform mesh with a first-order approximation and an equilibrium (resp., fine) model for the hpm-adaptation (resp., hp-adaptation), a fixed fraction of 25% of the mesh elements is selected for refinement at each step for both adaptations (step 1 of Algorithm 2).

As a validation of the error estimates, we first consider a linear flux, $f(v) = -v$, and impose a discontinuous relaxation rate: $\varepsilon(x) = 1$ if $x < 2$ and $\varepsilon(x) = 1/1000$ if $x > 2$. This configuration leads to the existence of an interface layer of small extent at the right of the discontinuity. The evolution of the error on J and of the error representation (4.8b) during the adaptation process are given in Figure 2 and are compared to results from hp-adaptation. We observe that including the model adaptivity lowers the number of DOFs for a given accuracy, while (4.8b) is seen to constitute a fair and efficient estimate of the true error. Figure 2 also indicates that (4.8b) is quadratic with respect to the L_2-norm of the error on the solution as stated in Theorem 5, which in turn confirms that the discretization and model errors are balanced (see the order of approximation of the remainder in (4.8a)).

We now consider the nonlinear Burgers' flux, $f(v) = \frac{v^2}{2}$, with a uniform relaxation rate: $\varepsilon \equiv 20$. The results are depicted in Figures 3 and 4. Again, we observe similar trends and confirm the better efficiency of the hpm-adaptation compared to the hp-adaptation. For the sake of comparison, we provide results obtained with m-adaptation only on a grid refined at the left boundary with a fourth-order discretization. The efficiency of m-adaptation is strongly dependent on the space discretization and thus requires a priori knowledge of the flow features, which represents a drawback compared to hpm-adaptation techniques.

The final solution of the hpm-adaptation process is given in Figure 4, where we see that the boundary and coupling conditions of the adjoint problem (3.13) are satisfied in a weak sense. In particular, the adjoint solution is continuous across the interface between different models. The equilibrium model is used on the left part of the domain during the adaptation process where the solution is indeed close to equilibrium. We
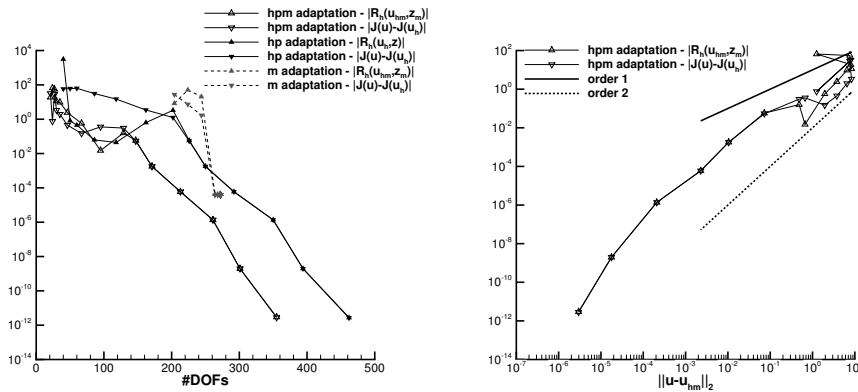
FIG. 2. *Linear flux with discontinuous ε. Evolution of the error* (1.1) *and error estimators* (4.8b)*: (left) at each adaptation step compared to hp-adaptation; (right) with respect to the error on the solution.*
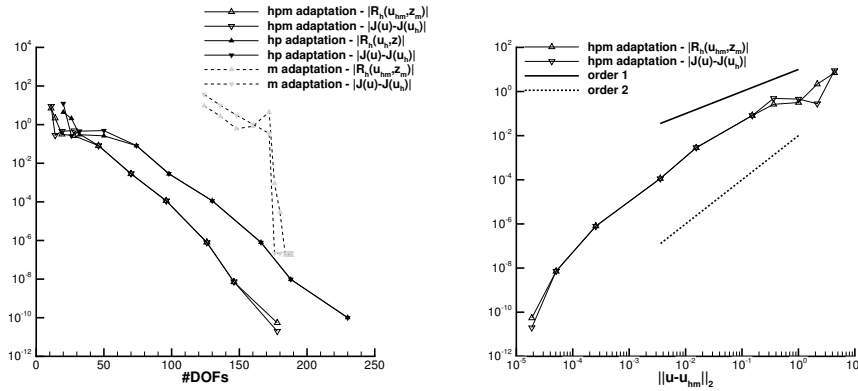

FIG. 3. *Burgers' flux with uniform ε. Evolution of the error* (1.1) *and error estimators* (4.8b)*: (left) at each adaptation step compared to hp-adaptation; (right) with respect to the error on the solution.*

also observe a good resolution of the interface layer leading to hp refinement due to the presence of steep gradients of the solution.

Finally, we consider Burgers' flux with a discontinuous characteristic relaxation rate: $\varepsilon(x) = 1$ if $x < 2$ and $\varepsilon(x) = 1/100$ if $x > 2$. The results are depicted in Figure 5, and the final hpm-solution is shown in Figure 6 and leads to similar observations. The grid used for the m-adaptation is refined at the discontinuity in ε, $x = 2$. Note that across the interface layer at $x = 2$, $f'(v)$ changes sign so the interface becomes characteristic and the second condition in (3.13) no longer imposes the continuity of z^v as observed in Figure 6.

7. Concluding remarks. In this work, a posteriori estimators of the modeling and discretization errors are derived in the context of the discretization with a DG method of steady hyperbolic systems with stiff relaxation source terms. We consider a hierarchy of models where the fine model may tend toward an equilibrium model through relaxation mechanisms modelized by the source terms. The estimators rely
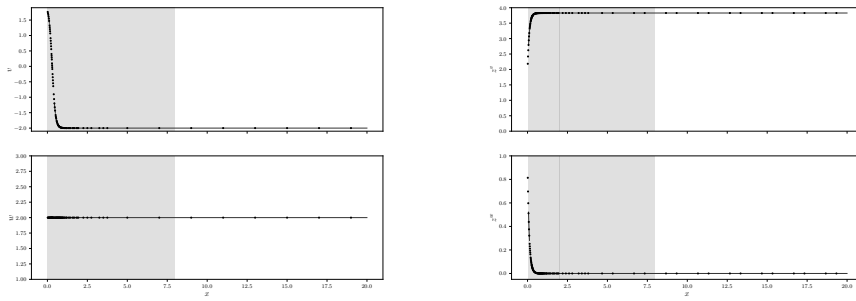
Fig. 4. *Burgers' flux with uniform ε. Final direct (left) and adjoint (right) solutions of the hpm-adaptation. In each element κ, the dots correspond to the values at $p_\kappa + 1$ points, while the gray (resp., white) zones indicate that the fine (resp., equilibrium) model is used.*
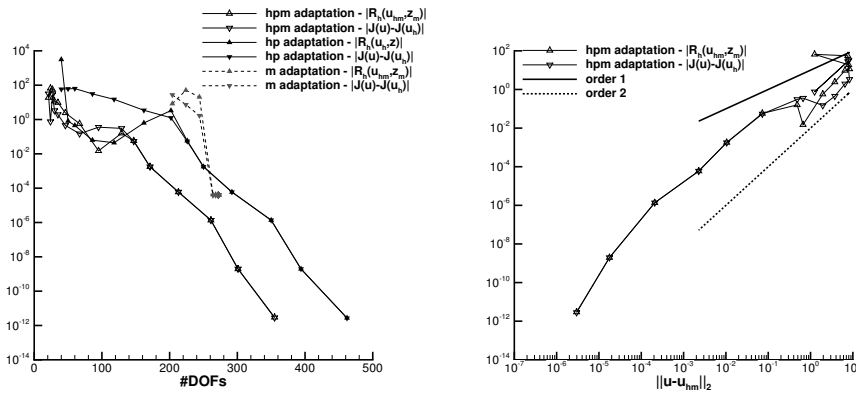

Fig. 5. *Burgers' flux with discontinuous ε. Evolution of the error (1.1) and error estimators (4.8b): (left) at each adaptation step compared to hp-adaptation; (right) with respect to the error on the solution.*
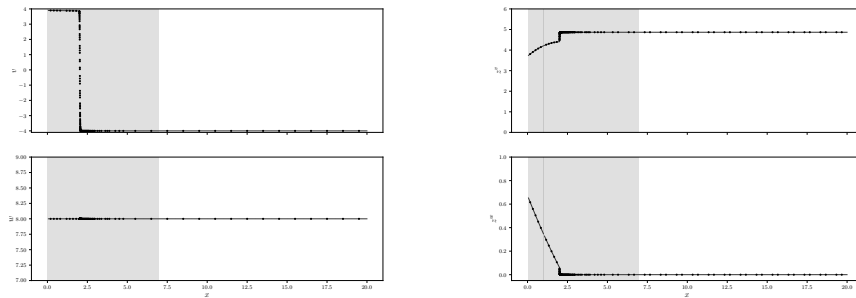

Fig. 6. *Burgers' flux with discontinuous ε. Final direct (left) and adjoint (right) solutions of the hpm-adaptation. In each element κ, the dots correspond to the values at $p_\kappa + 1$ points, while the gray (resp., white) zones indicate that the fine (resp., equilibrium) model is used.*

on an adjoint-based representation of both components of the error associated to a given functional of interest.

An adaptation algorithm is then proposed which aims at balancing both components of the error and tailoring the error on the functional of interest under a

prescribed tolerance. The local model refinement is performed by using the adapted model according to the associated error level. At interfaces of domains with different models, coupling conditions are applied through the solution of a Riemann problem in order to model the transfer of information. The positions of the interfaces are set by the respective positions of the models and may move during the adaptation. The discretization refinement is based on either an increase of the local order of the DG scheme or a local mesh subdivision according to a local indicator of the smoothness of the solution.

The present adaptation method has been successfully applied to the simulation of steady solution of a Jin–Xin relaxation system. Numerical experiments highlight the relevance of *hpm*-adaptation and sharpness of the error estimators as well as an improvement of the usual *hp*-adaptation by reducing the total number of DOFs of the discrete problem for a same error level. Future work will consider the application of this technique to a hierarchy of two-phase flow models.

Appendix A. The solution of the Riemann problem $\mathcal{W}_r^e(\cdot; \cdot, \cdot)$ associated to the coupling problem (2.14) has been solved in [21] when the flux function f is convex. We propose here a method for its resolution for a $\mathcal{C}^1$ flux function. A similar result stands for $\mathcal{W}_e^r$ and may be easily deduced from the results below.

By $\mathbf{u}_L = (v_L, w_L)^\top$ we denote the state variable on $x < 0$ at $t = 0$ and v_R the initial state variable on $x > 0$ and further define

$$\mathbf{u}^- = (v^-, w^-)^\top := \mathcal{W}_r^e(0^-; \mathbf{u}_L, v_R), \quad \mathbf{u}^+ = (v^+, w^+)^\top := \mathcal{W}_r^e(0^+; \mathbf{u}_L, v_R),$$

where $w^+ = f(v^+)$ and (2.15) gives $w^- = w^+ = f(v^+)$. Then, a contact wave of speed $-a$ separates the states $\mathbf{u}_L$ and $\mathbf{u}^-$ in the left region. The Rankine–Hugoniot condition gives

$$av_L + w_L = av^- + w^-,$$

and v^+ should be the right limit of the half Riemann problem (for $x > 0$, $t > 0$) defined by

(A.1) $$\partial_t v + \partial_x f(v) = 0, \quad v(0, t) \overset{BLN}{=} v^-, \quad v(x, 0) = v_R.$$

We denote $\mathcal{W}_{\frac{1}{2}}(\frac{x}{t}; v^-, v_R)$ the solution to (A.1) and $\mathcal{W}(\frac{x}{t}; v^-, v_R)$ the solution to the customary Riemann problem

$$\partial_t v + \partial_x f(v) = 0, \quad \forall x > 0, t > 0, \quad v(x, t = 0) = \begin{cases} v^- & \text{if } x < 0, \\ v_R & \text{if } x > 0. \end{cases}$$

Since the states v^- and v_R are constant, the solution to (A.1) has an extension as an entropy solution of the customary Riemann problem [20]:

$$\mathcal{W}_{\frac{1}{2}}(\xi; v^-, v_R) = \mathcal{W}(\xi; v^-, v_R) \quad \forall \xi > 0$$

and is thus easily solved for scalar equations [37]:

$$f\big(\mathcal{W}_{\frac{1}{2}}(0^+; v^-, v_R)\big) = \begin{cases} \displaystyle\min_{v^- \leq \theta \leq v_R} f(\theta) & \text{if } v^- \leq v_R, \\ \displaystyle\max_{v_R \leq \theta \leq v^-} f(\theta) & \text{if } v_R < v^-. \end{cases}$$

We then have the following result.

THEOREM 7. *For data v_L, w_L, and v_R in $\mathcal{U}$ defined in* (A.3), *the coupling Riemann problem has a unique entropy solution:*

$$\mathcal{W}_r^e\left(\xi; \mathbf{u}_L, v_R\right) = \begin{cases} \mathbf{u}_L, & \xi < -a, \\ \left(v^-, f\left(\mathcal{W}(0^+; v^-, v_R)\right)\right)^\top, & -a < \xi < 0, \\ \left(\mathcal{W}(\xi; v^-, v_R), f\left(\mathcal{W}(\xi; v^-, v_R)\right)\right)^\top, & 0 < \xi, \end{cases}$$

where v^- is the unique solution to the equation

(A.2)
$$v^- = v_L + \frac{w_L - f\left(\mathcal{W}(0^+; v^-, v_R)\right)}{a}.$$

Proof. Consider the function

$$g : I \ni v \mapsto g(v) = a(v - v_L) - w_L + f\left(\mathcal{W}(0^+; v, v_R)\right).$$

Thus, v^- is the solution to the equation $g(v) = 0$. As g is strictly increasing according to the subcharacteristic condition (2.13), if v^- exists, it is unique. To guarantee the existence we should have $g(v_m) < 0$ and $g(v_M) > 0$, where v_m and v_M have been defined in subsection 2.3:

$$\begin{cases} g(v_m) < 0 & \iff & w_L > a(v_m - v_L) + \inf_{v_m \le \theta \le v_R} f(\theta) =: H_m(v_L, v_R), \\ g(v_M) > 0 & \iff & w_L < a(v_M - v_L) + \sup_{v_R \le \theta \le v_M} f(\theta) =: H_M(v_L, v_R). \end{cases}$$

It defines the set of admissible states to where (v_L, w_L, v_R) should belong:

(A.3)
$$\mathcal{U} := \left\{ (v_L, w_L, v_R) \in I \times f(I) \times I : H_m(v_L, v_R) < w_L < H_M(v_L, v_R) \right\}. \qquad \square$$

From the mean value theorem and (2.13), we establish that

$$f(v_m) - f(v_L) < a(v_L - v_m), \quad f(v_L) - f(v_M) < a(v_M - v_L),$$

so that $H_m(v_L, v_R) < f(v_L) < H_M(v_L, v_R)$ and $\mathcal{U}$ is nonempty. Note that if $\inf f(I) = f(v_m)$ and $\sup f(I) = f(v_M)$, then $\mathcal{U}$ is simply $I \times f(I) \times I$.

The solution of the Riemann problem is then obtained by solving (A.2) for v^- with a root-finding algorithm.

REFERENCES

[1] N. AGUILLON AND R. BORSCHE, *Numerical Approximation of Hyperbolic Systems Containing an Interface*, preprint, arXiv:1603.05372 [math.NA], 2016.

[2] A. AMBROSO, C. CHALONS, F. COQUEL, T. GALIÉ, E. GODLEWSKI, P.-A. RAVIART, AND N. SEGUIN, *The drift-flux asymptotic limit of barotropic two-phase two-pressure models*, Commun. Math. Sci., 6 (2008), pp. 521–529.

[3] A. AMBROSO, C. CHALONS, F. COQUEL, E. GODLEWSKI, F. LAGOUTIÈRE, P.-A. RAVIART, AND N. SEGUIN, *The coupling of homogeneous models for two-phase flows*, Int. J. Finite Vol., 4 (2007), pp. 1–39.

[4] A. AMBROSO, J.-M. HÉRARD, AND O. HURISSE, *A method to couple HEM and HRM two-phase flow models*, Comput. Fluids, 38 (2009), pp. 738–756.

[5] M. R. BAER AND J. W. NUNZIATO, *A two-phase mixture theory for the deflagration-to-detonation transition (ddt) in reactive granular materials*, Int. J. Multiphase Flow, 12 (1986), pp. 861–889.

[6] C. BARDOS, A.-Y. LEROUX, AND J.-C. NÉDÉLEC, *First order quasilinear equations with boundary conditions*, Comm. Partial Differential Equations, 4 (1979), pp. 1017–1034.

[7] R. Becker and R. Rannacher, *An optimal control approach to a posteriori error estimation in finite element methods*, Acta Numer., 10 (2001), pp. 1–102.

[8] C. Bernardi, T. Chacón Rebollo, F. Hecht, and R. Lewandowski, *Automatic insertion of a turbulence model in the finite element discretization of the Navier-Stokes equations*, Math. Models Methods Appl. Sci., 19 (2009), pp. 1139–1183.

[9] M. Braack and A. Ern, *A posteriori control of modeling errors and discretization errors*, Multiscale Model. Simul., 1 (2003), pp. 221–238.

[10] C. Cancès, F. Coquel, H. Mathis, E. Godlewski, and N. Seguin, *Error analysis of a dynamic model adaptation procedure for nonlinear hyperbolic equations*, Commun. Math. Sci., 14 (2016), pp. 1–30.

[11] G.-Q. Chen, C. D. Levermore, and T.-P. Liu, *Hyperbolic conservation laws with stiff relaxation terms and entropy*, Comm. Pure Appl. Math., 47 (1994), pp. 787–830.

[12] F. Coquel, E. Godlewski, K. Haddaoui, C. Marmignon, and F. Renac, *Choice of measure source terms in interface coupling for a model problem in gas dynamics*, Math. Comp., 85 (2016), pp. 2305–2339.

[13] F. Coquel, S. Jin, J.-G. Liu, and L. Wang, *Well-posedness and singular limit of a semilinear hyperbolic relaxation system with two-scale relaxation rate*, Arch. Ration. Mech. Anal., 214 (2014), pp. 1051–1084.

[14] P. Degond, G. Dimarco, and L. Mieussens, *A moving interface method for dynamic kinetic-fluid coupling*, J. Comput. Phys., 227 (2007), pp. 1176–1208.

[15] F. Dubois and P. Le Floch, *Boundary conditions for nonlinear hyperbolic systems of conservation laws*, J. Differential Equations, 71 (1988), pp. 93–122.

[16] K. J. Fidkowski and P. L. Roe, *An entropy adjoint approach to mesh refinement*, SIAM J. Sci. Comput., 32 (2010), pp. 1261–1287.

[17] J. Giesselmann and T. Pryer, *A posteriori analysis for dynamic model adaptation in convection-dominated problems*, Math. Models Methods Appl. Sci., 27 (2017), pp. 2381–2423.

[18] M. B. Giles and N. A. Pierce, *Analytic adjoint solutions for the quasi-one-dimensional Euler equations*, J. Fluid Mech., 426 (2001), pp. 327–345.

[19] M. B. Giles and E. Süli, *Adjoint methods for PDEs: A posteriori error analysis and post-processing by duality*, Acta Numer., 11 (2002), p. 145–236.

[20] E. Godlewski and P.-A. Raviart, *Numerical Approximation of Hyperbolic Systems of Conservation Laws*, Appl. Math. Sci. 118, Springer, New York, 1996.

[21] K. Haddaoui, *Méthodes Numériques de Haute Précision et Calcul Scientifique pour le Couplage de Modèles Hyperboliques*, Ph.D. thesis, Université Pierre et Marie Curie, Paris, 2016.

[22] R. Hartmann, *Adjoint consistency analysis of discontinuous Galerkin discretizations*, SIAM J. Numer. Anal., 45 (2006), pp. 2671–2696.

[23] R. Hartmann and P. Houston, *Adaptive discontinuous Galerkin finite element methods for nonliner hyperbolic conservation laws*, SIAM J. Sci. Comput., 24 (2002), pp. 979–1004.

[24] R. Hartmann and P. Houston, *Adaptive discontinuous Galerkin finite element methods for the compressible Euler equations*, J. Comput. Phys., 183 (2002), pp. 508–532.

[25] R. Hartmann and T. Leicht, *Generalized adjoint consistent treatment of wall boundary conditions for compressible flows*, J. Comput. Phys., 300 (2015), pp. 754–778.

[26] P. Houston, *Adjoint error estimation and adaptivity for hyperbolic problems*, in Handbook of Numerical Methods for Hyperbolic Problems 18, R. Abgrall and C.-W. Shu, eds., Elsevier, Amsterdam, 2017, pp. 233–261.

[27] S. Jin and Z. Xin, *The relaxation schemes for systems of conservation laws in arbitrary space dimensions*, Comm. Pure Appl. Math, 48 (1995), pp. 235–277.

[28] M. G. Larson and T. J. Barth, *A posteriori error estimation for adaptive discontinuous Galerkin approximations of hyperbolic systems*, in Discontinuous Galerkin Methods: Theory, Computation and Applications, B. Cockburn, G. E. Karniadakis, and C.-W. Shu, eds., Springer, Berlin, 2000, pp. 363–368.

[29] P. Lesaint and P.-A. Raviart, *On a finite element method for solving the neutron transport equation*, in Mathematical Aspects of Finite Elements in Partial Differential Equations, Academic Press, New York, 1974, pp. 89–123.

[30] H. Lund, *A hierarchy of relaxation models for two-phase flow*, SIAM J. Appl. Math., 72 (2012), pp. 1713–1741.

[31] A. Majda, *The stability of multidimensional shock fronts*, Mem, Amer. Math. Soc., 41 (1983), pp. 1–96.

[32] H. Mathis, C. Cancès, E. Godlewski, and N. Seguin, *Dynamic model adaptation for multiscale simulation of hyperbolic systems with relaxation*, J. Sci. Comput., 63 (2015), pp. 820–861.

[33] A. Murrone and P. Villedieu, *Numerical modeling of dispersed two-phase flows*, Aerospace-Lab J., 2 (2011), pp. 34–46.

[34] R. Natalini, *Convergence to equilibrium for the relaxation approximations of conservation laws*, Comm. Pure Appl. Math., 49 (1996), pp. 795–823.

[35] J. Oden and K. S. Vemaganti, *Estimation of local modeling error and goal-oriented adaptive modeling of heterogeneous materials*, J. Comput. Phys., 164 (2000), pp. 22–47.

[36] J. T. Oden and S. Prudhomme, *Estimation of modeling error in computational mechanics*, J. Comput. Phys., 182 (2002), pp. 496–515.

[37] S. Osher, *Riemann solvers, the entropy condition, and difference approximations*, SIAM J. Numer. Anal., 21 (1984), pp. 217–235.

[38] N. A. Pierce and M. B. Giles, *Adjoint and defect error bounding and correction for functional estimates*, J. Comput. Phys., 200 (2004), pp. 769–794.

[39] W. H. Reed and T. R. Hill, *Triangular Mesh Methods for the Neutron Transport Equation*, Technical report LA-UR-73-479, Los Alamos Scientific Laboratory, Los Alamos, NM, 1973.

[40] J. Schütz, S. Noelle, C. Steiner, and G. May, *A note on adjoint error estimation for one-dimensional stationary balance laws with shocks*, SIAM J. Numer. Anal., 51 (2013), pp. 126–136.

[41] E. Stein and S. Ohnimus, *Anisotropic discretization- and model-error estimation in solid mechanics by local Neumann problems*, Comput. Methods Appl. Mech. Engrg., 176 (1999), pp. 363–385.

[42] S. Ulbrich, *A sensitivity and adjoint calculus for discontinuous solutions of hyperbolic conservation laws with source terms*, SIAM J. Control Optim., 41 (2002), pp. 740–797.